Final report on: New CO2 capture materials based on nano sized oxide particles

Prepared by: A.M. Frey

Reviewed by: P.D. Cobden

Approved by: J.Brouwer
(CATO-2 Director)

1 Executive Summary (restricted)

Two major opportunities were identified for improving the cyclic stability and capacity of bulk oxide based high temperature capture sorbent: the role of trace elements on the structure-activity-deactivation of CaO with the implicit tailoring of bulk materials, and the interaction of steam in the structure-activity relationship.

Steam reactivation is as a method of improving cyclic performance of Ca-based system. This study was carried out in order to elucidate the structure-activity-relationship in the CaO-$Ca(OH)_2$-$CaCO_3$ system. The results show that the best reactivation of the Ca-based sorbent is gained when stoichiometric amounts of H_2O compared to Ca are used. The utilisation of Ca by CO_2 improves by nearly 50% under these conditions, but the overall utilisation of Ca remains relatively low at 30%. This means a relatively large amount of steam is required per gain in sorbent capacity, which diminishes the value of steam reactivation for improving cyclic performance.

The structure activity relationship of for bulk high surface area CaO and Mg-modified MgO-CaO materials was investigated in order to evaluate the role of Mg in changing the properties of these CO_2 adsorption materials for CO_2 capture under different conditions. Magnesium seems to have a promising effect for stability and the possibility for regeneration for sorbent prepared with the sol gel method, but when impregnating it to commercial CaO it has no stabilizing effect. The location of Mg must thus be considered crucial for the impact on the performance of CaO CO_2 capture materials, and this lead the project to take a more fundamental look at the interaction of CaO with possible supports.

As a support, zirconia is one of the most interesting for CaO used in post combustion applications. The preparation method is important for the distribution of strong/weak base sites and thus for de desorption of CO_2 important for regeneration. However, desorbing CO_2 at too high temperature (800 °C and higher) the material properties changes (phase transition) and the CO_2 capacity decreased. It is thus important to optimize the regeneration condition for CO_2 desorption in isothermal period of 600-700 °C.

The project has increased the knowledge of CaO-based material with both H_2O and CO_2 under post combustion conditions, and how support and dopants effect the structural-reactivity relationship. Of the solutions available, the use of steam to increase the cyclic capacity of these materials would seem to be the most applicable for near term use, unless new system configurations can be devised to take advantage of the cyclic capacity of zirconia supported materials below their transition point.

Distribution List

(this section shows the initial distribution list)

External	copies	Internal	Copies
Harry Bitter	1	Paul Cobden	1
Anne Mette Frey	1	Wim Haije	1
Krijn de Jong	1	Daan Jansen	1
Hans Geerlings	1		

Document Change Record

(this section shows the historical versions, with a short description of the updates)

Version	Nr of pages	Short description of change	Pages

Table of Content

1 Executive Summary (restricted) 2
2 Applicable/Reference documents and Abbreviations 4
2.1 Applicable Documents 4
2.2 Reference Documents 4
2.3 Abbreviations 4
3 Final Report on quantitative structure-activity relationships for nano-sized oxide particles and CO_2 capture properties; New material for Post-combustion capture of CO_2 5
3.1 Steam Reactivation of CaO-based Sorbents for CO_2 capture 5
3.1.1 Introduction 5
3.1.2 Experimental 6
3.1.3 Results and Discussion 8
3.1.4 Applicability to Power Generation 13
3.1.5 Other issues 13
3.1.6 Conclusions 14
3.1.7 References 14
3.2 CaO and Mg promoted CaO as post combustion CO_2 capture materials 17
3.2.1 Goal 17
3.2.2 Material prepared by sol gel methods: 17
3.2.3 XRD and Rietveld analysis 19
3.2.4 TEM analysis 20
3.2.5 DFT 21
3.2.6 Performance of the materials for CO_2 capture 21
3.2.7 References 25
3.3 Calcium oxide supported on zirconia as CO_2 capture materials 26
3.3.1 Introduction and aim 26
3.3.2 Preparation of materials 26
3.3.3 Results and discussion 29
3.3.4 Conclusions 41
3.4 Summary and Conclusions 44

2 Applicable/Reference documents and Abbreviations

2.1 Applicable Documents

(Applicable Documents, including their version, are documents that are the "legal" basis to the work performed)

	Title	Doc nr	Version
AD-01d	Toezegging CATO-2b	FES10036GXDU	2010.08.05
AD-01f	Besluit wijziging project CATO2b	FES1003AQ1FU	2010.09.21
AD-02a	Consortium Agreement	CATO-2-CA	2009.09.07
AD-02b	CATO-2 Consortium Agreement	CATO-2-CA	2010.09.09
AD-03g	Program Plan 2013b	CATO2-WP0.A-D03	2013.04.01

2.2 Reference Documents

(Reference Documents are referred to in the document)

	Title	Doc nr	Issue/version	date

2.3 Abbreviations

(this refers to abbreviations used in this document)

CCS	Carbon Capture and Sequestration
PC	Pulverised coal power plant
Oxyfuel	Oxyfuel power plant
IGCC	Integrated Gasification combined Cycle
NGCC	Natural Gas Combine Cycle
MFC	Mass Flow Controller
SSA	Specific Surface Area
BET	Brunauer, Emmett and Teller
XRD	X-ray diffraction
TEM	Transmission Electron Microscope
EDX	Energy-Dispersive X-ray Spectroscopy
DFT	Density Functional Theory
TPD	Temperature Programmed Desorption

3 Final Report on quantitative structure-activity relationships for nano-sized oxide particles and CO_2 capture properties; New material for Post-combustion capture of CO_2.

3.1 Steam Reactivation of CaO-based Sorbents for CO_2 capture

Paul Cobden, Gerard Elzinga & Wim Haije

3.1.1 Introduction

Deactivation of Ca-based sorbents is a well-known phenomenon when used in both post-combustion and pre-combustion settings [1-2], and therefore has a profound effect on the economics of the use of such materials in looping cycles for CO_2 capture [3]. Several methods of improving cyclic capacity have been suggested in the literature. This list is not exhaustive, but highlight steam reactivation [4] and super heating [5-6]. In pre-combustion CaO-looping it has been shown that at least 15% of the cyclic capacity must be retained in order to gain maximum thermodynamic efficiency in a power cycle [7]. These properties were later demonstrated to be a property of a commercially available material [8]. This was later reported to be a linked to small amounts of trace elements in this material, which improving the stability [9]. Stabilisation of naturally occurring Ca-containing materials through cheap processing steps has been a goal of many groups, e.g. [10-11], although substantially more groups have been working on completely synthetic sorbents, e.g. [12-20] a small selection from 2010 alone.

The focus on synthetic sorbents would seem somewhat misplaced and mainly of academic interest considering the afore mentioned economic incentives to use materials based on natural sources with a minimum of processing [3]. However, for applications using natural gas for H_2 production and not power production with CO_2 capture, there could be a market for these synthetic materials. Even so, there is no immediately apparent literature in which testing is performed under realistic conditions for H_2 production, mainly these groups perform testing at low pressure conditions associated with clean post-combustion conditions. Under such post-combustion conditions, the interaction with sulphur is largely ignored, although this is not always the case [14,21-22]. Once sulphate is formed with these materials, the Ca-centres associated with that sulphate are effectively taken out of the system and must be replaced. The amount of sulphur in the fuel effectively dictates the sorbent replacement rate in the very best case, i.e. without deactivation. It is therefore easy to imagine that synthetic post-combustion sorbent will be economically unviable.

In a similar sense, when looking at pre-combustion scheme involving H_2 production, testing is hardly ever done under realistic high pressure conditions. It has been known for a long time that high pressure, especially with respect to $SO_x > CO_2 > H_2O$ effectively lead to increased sintering of the CaO materials [23]. There are only a few CaO looping projects that require H_2 at low pressure, e.g. [24], whereas most assume high pressure operation, e.g. [7, 25-26]. Unpublished results show that sintering under high pressure, and thus loss of cyclic capacity, can be very dramatic under typical pre-combustion conditions [27].

Given the current state of both pre- and post-combustion sorbent development in CaO-$CaCO_3$ looping this provides two channels for producing distinctive work on understanding these systems in order to work around the problems present. The first is to determine how effective steam reactivation is in terms of optimum temperatures and exposures to steam. This can be easily compared to previous work on system studies, where it was shown that steam consumption must be less than 7 mol H_2O divided over the sum of the carbon in the fuel and the carbon in the CO_2 exhaust [25], in order to avoid situations where extra fuel is burnt solely for production of high temperature steam needed in the process. The consumption had to be considerably lower to provide a system with a suitable efficiency. The second line of work to be explored is the fact that stabilisation of CaO has been reported when low levels of trace elements are present [9]. This phenomenon has been noted, but there is a lack of understanding into how this process could work and thus how to optimise this process to modify naturally occurring minerals to improve their capacities and lifetimes. The focus of this report is the effect of rehydration of the capacity of known sorbents, in order to establish if this is a viable method for increasing capacities and lifetimes, i.e. the first route as set out above.

This introduction has dealt almost exclusively with Ca-based sorbent, for which there are several good recent reviews [28-29]. Other alkaline- and alkali-based materials could also be interesting for use as sorbents in these processes, e.g. Mg [30-34] and Ba [35-36]. Considering the stabilisation effect of Mg on Ca-based sorbent it is prudent to look at the other possible combination available. This will be addressed at a later stage.

3.1.2 Experimental

A fully automated test-rig for catalyst and sorption research purposes was employed for the investigation of hydration on capacity of Ca-based material. The system used Wizcon software to control all flows, temperatures and valve positions. Experimental programs were set up for the complete experiments; these experimental programs could be made in Microsoft Excel.
Figure 1 is a representation of the entire system. A range of mass flow controllers, MFCs (Bronkhorst) formed the basis of the system. After each controller an extra solenoid valve was installed in order to prevent small leakages of the MFCs into the system. A combination of a liquiflow and CEM unit (Bronkhorst) were used to add steam to the gas mixture. Two 3-way solenoid valves were used to pass the feed gas over the reactor or to bypass it. The gas flow in the direction of the reactor passed a 4-way valve which could used to change the gas direction in the reactor, and thus to perform desorption in a counter flow mode. A carbonyl trap consisting of a small piece of stainless steel tubing at 250°C was present in the system to remove nickel carbonyl ($Ni(CO)_4$) which might be present when CO is used. A stainless steel oven with ceramic inserts was used in which a quartz reactor could be placed. The outlet of the reactor was connected to a gas dryer (Perma Pure) to remove steam before entering the analysis section. Gas analysis was performed with both Micro GC (HP) and an Uras 14 CO_2 analyzer (Hartmann & Braun).

A typical hydration experimental sequence is shown in ***Figure 2***. Initially a $CO_2/N_2/H_2O$ mixture was prepared bypass the reactor, to diminish the effects of transients in concentration, and to ensure a stabilised steam flow. The sorbent was then exposed to this mixture at the adsorption temperature (600-650°C) for 1hr in most cases; this is sufficient to ensure breakthrough of CO_2 in the column. The flow was changed to N_2/H_2O only and the system heated to the desorption temperature (800-850°C). The regeneration temperature was held for 1 hr, and then the temperature was lowered to the adsorption temperature. This set of adsorption-desorption cycles was repeated several times.

The concentration of CO_2 used in these experiments was 15% as a representative value for CO_2 concentration in coal based power plants flue gas. The concentration of H_2O was 29% during both hydration and loading parts of the cycle.

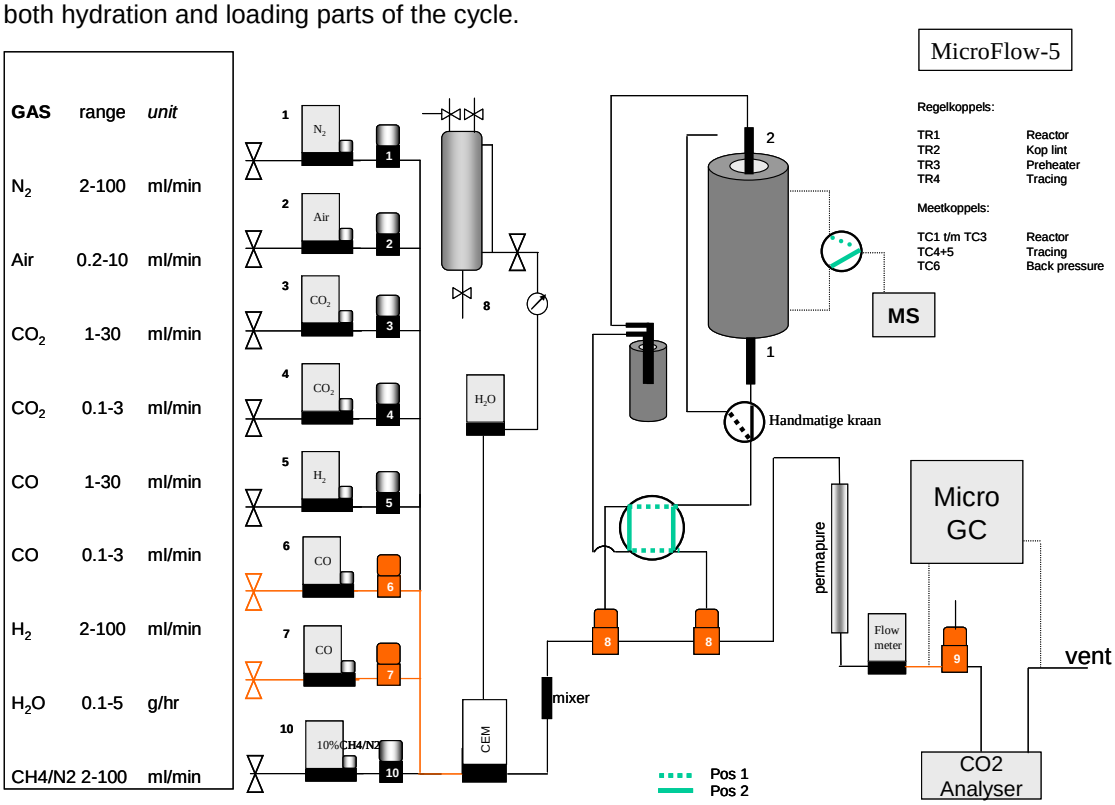

Figure 1 *Schematic representation of the experimental set-up for CO_2 capacity measurements.*

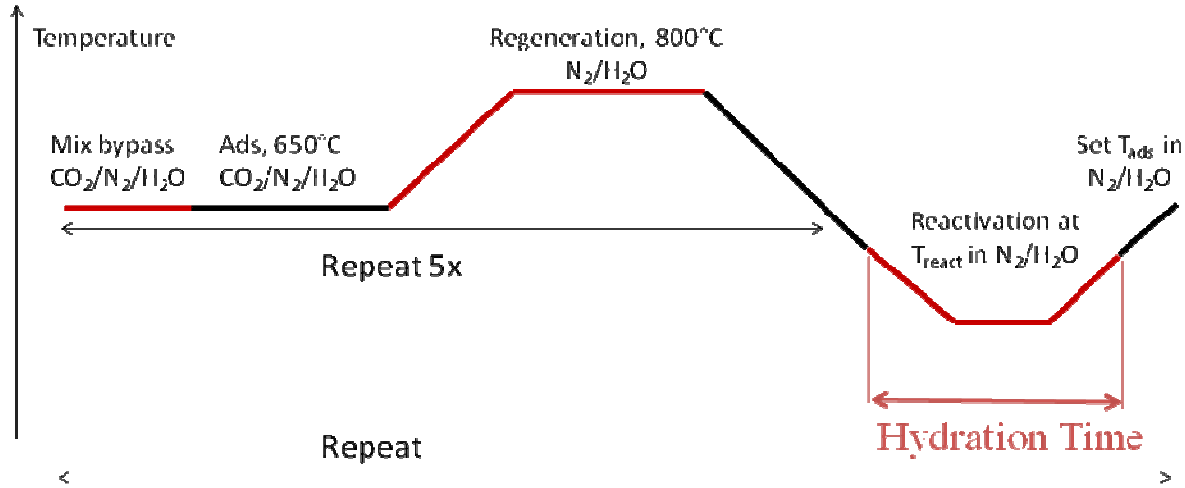

Figure 2 *Schematic representation of the cyclic treatment of Ca-based sorbent with steam hydration*

Every 5 cycles, after the end of desorption stage, the temperature was lowered in the N_2/H_2O mixture to the chosen hydration temperature (300-450°C) for a specific amount of time. The time chosen ranged for the specific amount of time to dose the stoichiometric equivalent between 0-5 mol steam per mol Ca in the sorbent. Subsequently the following set of five adsorption-desorption cycles was performed. The capacities were calculated on the basis of the breakthrough data.

3.1.3 Results and Discussion

Figure 3 shows an example of three runs using different hydration times and temperature, and the effect it has on CO_2 capacity. It is clear to see that in the absence of hydration capacities drop quite rapidly as is known from the literature. The blue line (circle symbol) shows a series of hydrations at 400°C, with gradually decreasing exposure times. It is clear to see that although hydration does have a positive effect at this temperature the sorbent does not recover its full potential during the hydration step. The green line (diamond symbol) shows a similar procedure at 300°C using an extended hydration time (310 minutes). After a few hydration cycles the capacity starts to follow a repeating pattern with reactivation to a consistent level. In a third set of experiments, red line (triangle symbol) the hydration period was initially kept the same, while the temperature was increased from 300 to 500°C in steps of 50°C. It is clear to see that the hydration step has little effect above 450°C. Later in the same set, it is clear to see that hydration has an effect below 400°C and that activity can be stabilised when sufficient steam is introduced into the system.

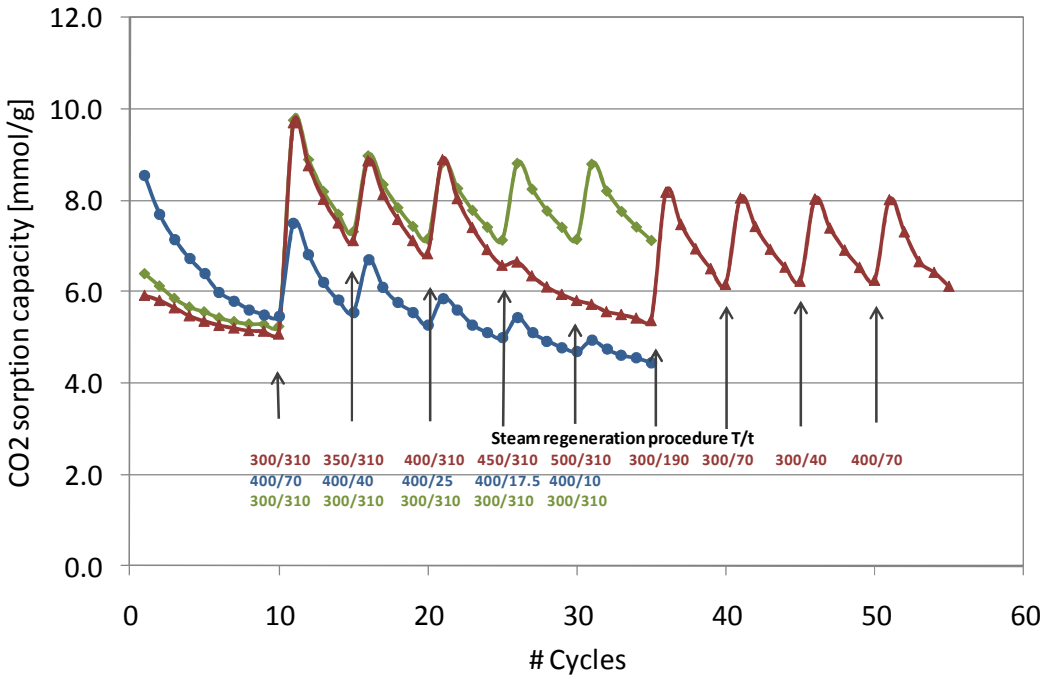

Figure 3 *Adsorption capacities as a function of cycle number. Regeneration points are marked with Hydration Temperature [°C]/ Hydration Time [min]. A stoichiometric 1:1 molar ratio H_2O:Ca is reached after 21 minutes.*

Thermodynamics of the CaO-H_2O-$Ca(OH)_2$ system reveal that at the chosen partial pressure of H_2O available in these experiments (0.29 bar), the temperature above which $Ca(OH)_2$ formation

should no longer possible is 460°C. This is slightly higher than the range above which hydration was no longer seen to be effective (see ***Figure 3***), but gives support to a hypothesis that $Ca(OH)_2$ formation may be critical in the regaining capacity during the hydration step.

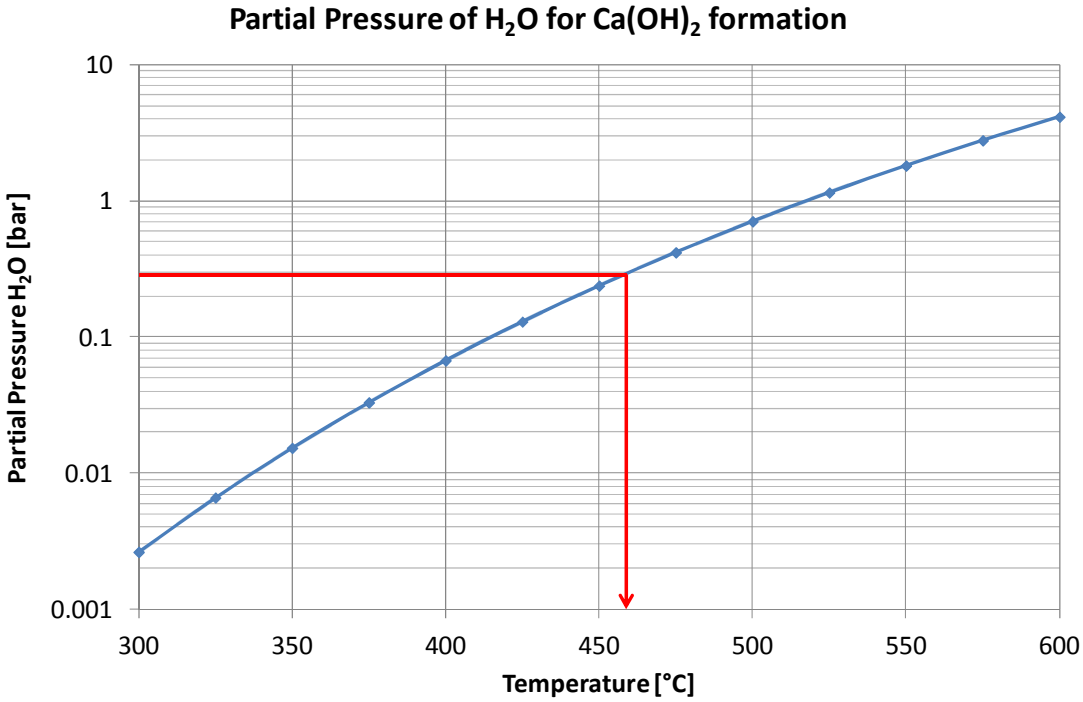

Figure 4 *Thermodynamic equilibrium partial pressure of H_2O required to form $Ca(OH)_2$ from CaO*

In a separate set of experiments (see ***Figure 5***) the effect of steam was monitored more closely. The red line (circle symbols) shows the effect of gradually decreasing the amount of steam used in hydration to zero (3rd hydration); this was done to see if the any possible strain effects on the CaO particles when cooling from 800 to 300°C also cause an increase in capacity. It could be imagined that thermal strain leads to formation of cracks in the material [37] given the ability of small amounts of Mg to affect the degradation behaviour of Ca-based materials [9]. Such cracking may lead to more surface area exposure leading to higher capacities. However, this would not seem to be the case here where the capacity continues to decrease when exposed only to N_2 at 300°C, and there only being a slight increase in capacity when exposed to N_2 only at 400°C. However, why any such strain effect would have a small effect at 400°C, and no effect at 300°C is difficult to reconcile with such a theory. The red line (circle symbols) also shows that capacity can be regained when the length of the hydration is increased. This is shown to more dramatic effect in Figure *6*, where the exposure time to H_2O is increased gradually, and full recovery in the cyclic changes in capacity is demonstrated.

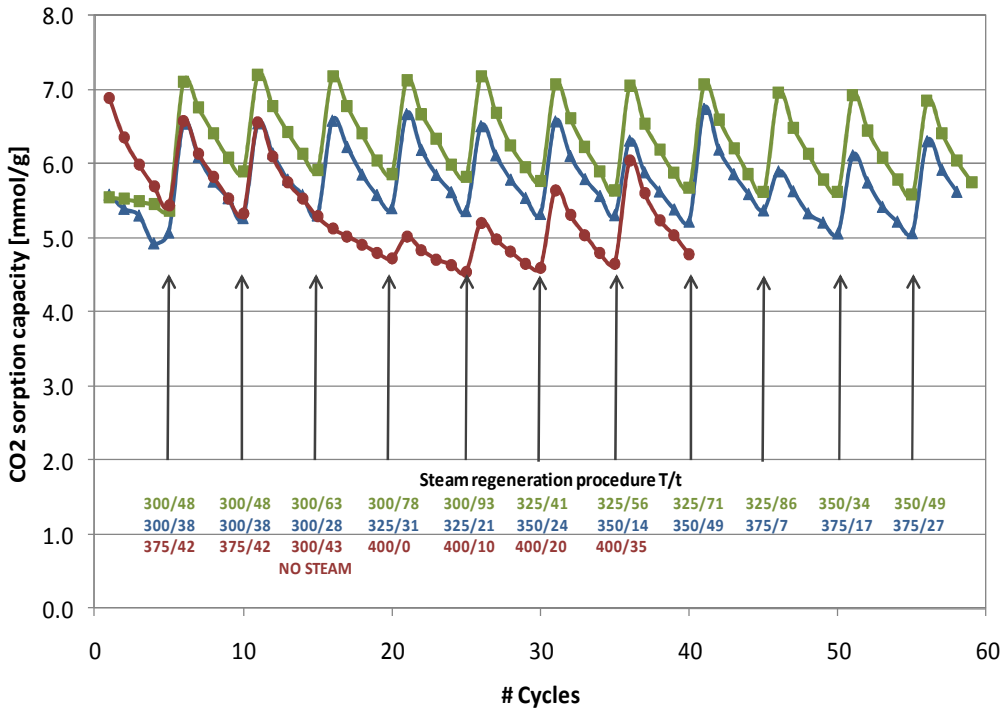

Figure 5 *Adsorption capacities as a function of cycle number. Regeneration point are marked with Hydration Temperature [°C]/ Hydration Time [min]. A stoichiometric 1:1 molar ratio H_2O:Ca is reached after 21 minutes.*

The effect of the length of steam hydration is also addressed in ***Figure 5*** in the green (square symbol) and blue (triangle symbol) experiments. At stoichiometric (and higher) steam additions the regeneration caused by hydration is the highest and relatively independent of temperature, except for temperatures above 400°C. In ***Figure 6***, the maximum increase in capacity after a hydration step is seen when the time chosen to regenerate, and the amount of steam dosed during that time is equal or greater than the stoichiometric amount of steam needed to fully convert all Ca present in the material into $Ca(OH)_2$. At higher steam dosages there is an increase in the overall capacity as the system reached a cyclic steady state, but not a large effect on the difference between capacity at the end of the five adsorption-desorption cycles and the capacity immediately following the hydration step.

The change in the capacity after the hydration step in summarised in ***Figure 7*** for a large number of experiments. The trend is clear here too, the largest jump in capacity is gained when a stoichiometric amount of steam is dosed to the system compared to the Ca present Depending on the temperature, the maximum is reached between 1-2 mol H_2O/mol Ca-content. Below this stoichiometric amount of steam there is a linear relationship between steam exposure and capacity jump. In one set of experiments the jump was higher than during other experiments, but the overall trend was the same, with a linear response in recovery versus steam until the stoichiometric amount has been dosed.

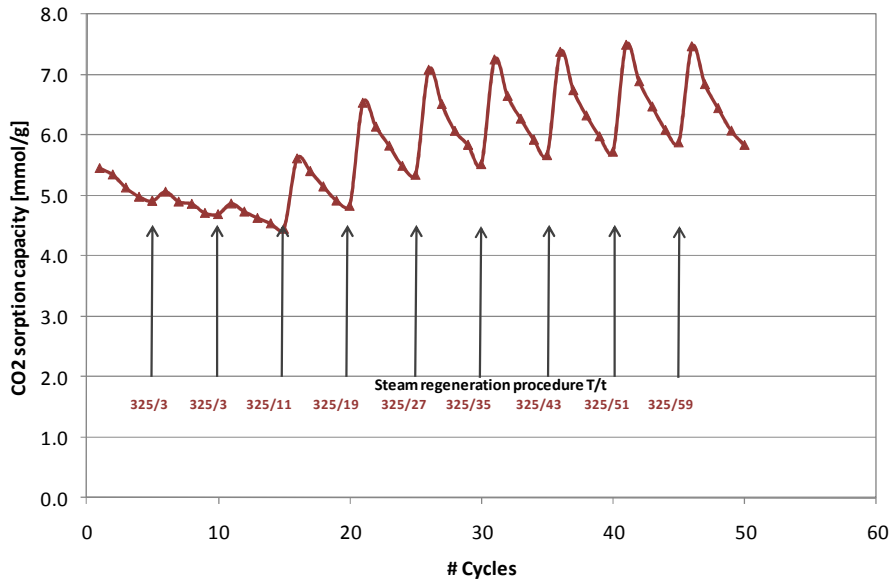

Figure 6 *Adsorption capacities as a function of cycle number. Regeneration point are marked with Hydration Temperature [°C]/ Hydration Time [min]. A stoichiometric 1:1 molar ratio H_2O:Ca is reached after 21 minutes.*

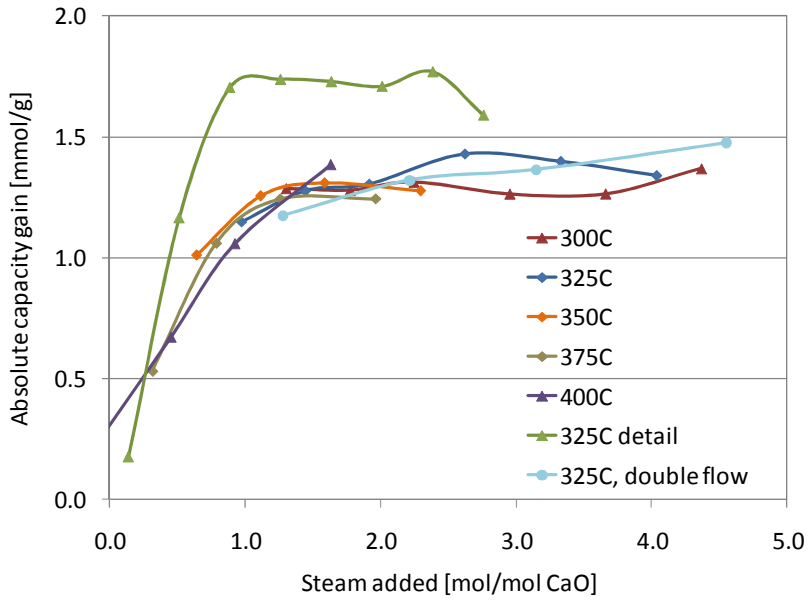

Figure 7 *Capacity jump after hydration step as function of the steam added during that hydration step compared to the capacity before the hydration step*

As the temperature increases the actual amount of steam needed also seems to increase. This can also be understood in terms of the thermodynamics of $Ca(OH)_2$ formation. From ***Figure 4***, at 400°C the thermodynamic slip of H_2O should be approximately 0.07 bar, which is approximately 25% of the dosed partial pressure of H_2O, i.e. 0.29 bar. Thus, for complete conversion, or the equivalent of complete conversion at 400°C, 33% more than the stoichiometric amount of steam per Ca must be dosed. Similarly at 325°C, where the thermodynamic slip of H_2O is very low (<0.007 bar), kinetics not limiting, virtually all the H_2O present can be used for conversion to $Ca(OH)_2$, and thus a stoichiometric amount of H_2O would be expected. The results follow the expected trend although there is significant error margin, and no in situ characterisations of materials were performed to verify the transformation into $Ca(OH)_2$. However, these assertions are supported by recent literature [38].

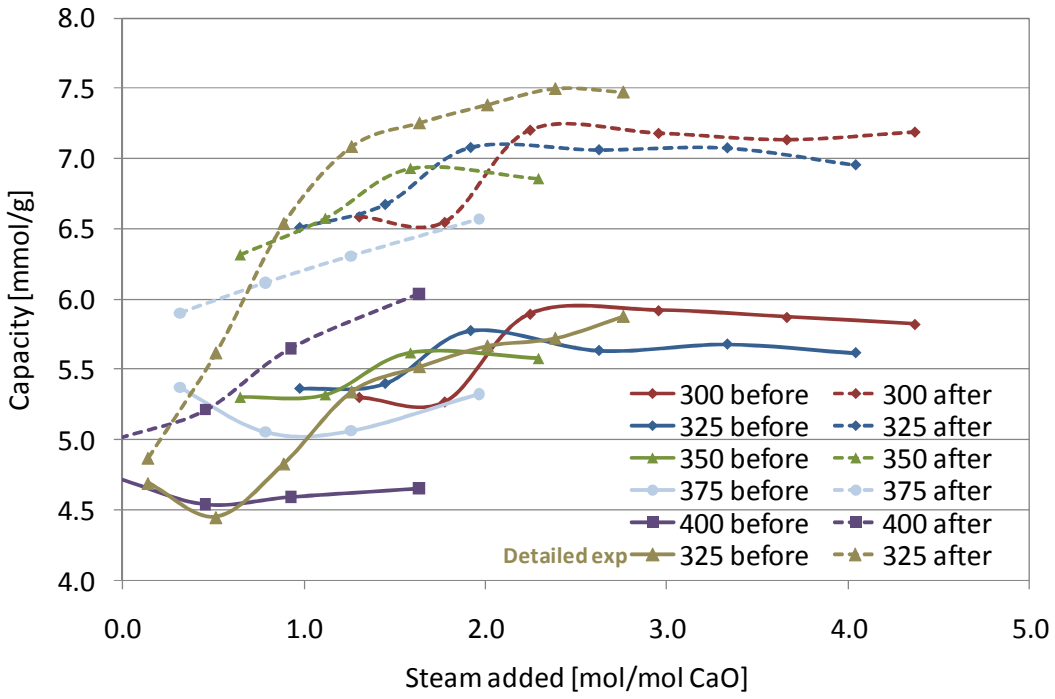

Figure 8 *Actual capacities as a function of stoichiometric addition of H_2O compared to Ca present in the sorbent and temperature,*

Finally, the actual capacities as a function of H_2O dosage and temperature is shown in ***Figure 8***. The best conditions for highest capacity found around 325°C, which also corresponds to the largest jump seen in cyclic capacity after hydration. There was also a slight improvement in overall capacity when cooling of the sorbent to hydration temperature was performed under dry conditions. This would seem to indicate that there is also a small role for the thermal shock of exposing a cooled sorbent to H_2O (an exothermic reaction ΔH = -109 kJ/mol), but that the conversion of CaO to $Ca(OH)_2$ the main driver is in improving cyclic capacity. It is however uncharacteristic that even though enough steam should be provided to cover complete conversion, the actual carrying capacity of the sorbent remains relatively low, at maximum 7.5 mmol/g compared to a maximum carrying capacity of 18 mmol/g.

3.1.4 Applicability to Power Generation

The results show clearly that regularly exposing the CaO material used for this test to steam can improve the capacity significantly. The average capacity in the cycles increased by approximately 50% compared to previous reports of the same material [9]. However, this still leaves overall utilisation of the sorbent at 30%, compared to 20% previously achieved. Effectively, this method of reactivation would require that 20% of the sorbent be regenerated at any time, and thus an extra steam usage of 2-4 mol steam per mol CO_2 extra recovered. Expressed in terms of total steam CO_2 recovery, the range is thus 0.67-1.33 mol steam per mol CO_2 avoided. This can be compared to results for other CCS technologies [39], as show in ***Table 1***.

Table 1 *Specific extra H_2O consumption for specific CCS technologies compared to base case*

Technology	Base case	Specific extra H_2O consumption per CO_2 avoided [mol/mol]	Reference
PC CCS	PC	1.19	[39]
Oxyfuel	PC	-0.15	[39]
IGCC CCS	PC	1.27	[39]
IGCC CCS	IGCC	1.05	[39]
CaO-Looping*	-	0.67-1.33	this work

* *excluding H_2O consumption during CO_2 compression, H_2O for fluidisation and H_2O makeup in a steam cycle connected to the steam cycle of the calcium looping reactor*

While it is clear that most CCS technologies can cause an increase in steam consumption (except for Oxyfuel) and that the extra steam consumption in the CaO-Looping system is, on face value, the same order. However, several factors are left out of this first screening that have been used in previous studies [39], which would indicate that steam consumption will be significantly higher in the case of CaO-looping. Firstly, H_2O is normally consumed in CO_2 compression train for interstage cooling. Secondly, H_2O will also be required for the fluidisation of seals and valves between the adsorber and calciner reactors. Thirdly, the CaO-looping system will have an associated steam cycle (for keeping the adsorber temperature at 600-650°), which will require H_2O makeup. The first is common to all CCS technologies, and is taken into account in the referenced work, and will only lead to a higher specific H_2O consumption in the case of CaO-looping. The second and third are specific and extra to CaO-looping. This oversimplified approach gives reason to believe that H_2O consumption in CaO-looping will be higher than in other CCS technologies. Of course a definitive answer can only be gained in a full analysis of the entire power train, but that is beyond the scope of this work.

3.1.5 Other issues

When these results are compared to previous results [9], it becomes clear that improvements in the overall stability of Ca-based materials can lead to much bigger gains, in terms of taking this technology further and keeping costs down, than adding complexity to the looping system. An extra hydration reactor system leads to a small gain in capacity at the expense of increasing H_2O consumption.

This ignores possible structural weakness of CaO particles that have been exposed to H_2O at the appropriate temperature [5-6,38] which would not work in its favour. This oversimplified analysis also ignores any kinetic effect that may be present causing higher reactivity of hydrated CaO

sorbent to CO_2. However, considering that the sorbent used start with an even higher capacity, and others have shown similar if not better carrying capacities [10-13], the stabilisation of this initial capacity represents a more important goal than the introduction of a new reactor concept.

This is not to say that hydration cannot play a role in these systems, but that stabilisation presents a more tangible manner of improving performance of CaO-based looping cycles. Therefore further work in work-package WP1.2F2 will be dedicated to understanding the decay mechanism of all alkaline-based metal oxide-carbonate looping cycles, and how this is affected by doping of other alkali/alkaline oxides.

3.1.6 Conclusions

It has been clearly demonstrated that steam hydration of a CaO-based material is effective in improving the carrying capacity of a sorbent. However the steam consumption needed for the extra capacity is not significantly lower than other CCS technologies and may even be substantially higher. Of the two methods for improving cyclic performance identified at the start of the project, i.e. steam hydration and doping, the focus of further work will be on the doping phenomenon. Steam hydration requires adding a steam equivalent of 1-2 moles steam per mol Ca present, which would correspond to complete conversion to $Ca(OH)_2$ during the hydration step. This however does not fully activate the Ca-based material as a maximum of only 30% of the Ca is available for CO_2 capture in the next cycle. The mechanistic understanding of how dopants improve long term stability would seem to offer more hope in understanding how these systems can be made more competitive.

3.1.7 References

[1] Silaban, A., & Harrison, D. P. (1995). High temperature capture of carbon dioxide: Characteristics of the reversible reaction between CaO(s) and CO2(g). *Chemical Engineering Communications, 137*, 177-190.

[2] Wang, J., & Anthony, E. J. (2005). On the decay behavior of the CO2 absorption capacity of CaO-based sorbents. *Industrial and Engineering Chemistry Research, 44*(3), 627-629.

[3] Abanades, J. C., Rubin, E. S., & Anthony, E. J. (2004). Sorbent cost and performance in CO2 capture systems. *Industrial and Engineering Chemistry Research, 43*(13), 3462-3466.

[4] Manovic, V., & Anthony, E. J. (2007). Steam reactivation of spent CaO-based sorbent for multiple CO2 capture cycles. *Environmental Science and Technology, 41*(4), 1420-1425.

[5] Materić, V., Edwards, S., Smedley, S. I., & Holt, R. (2010). Ca(OH)2 superheating as a low-attrition steam reactivation method for CaO in calcium looping applications. *Industrial and Engineering Chemistry Research, 49*(24), 12429-12434.

[6] Materić, B. V., Sheppard, C., & Smedley, S. I. (2010). Effect of repeated steam hydration reactivation on CaO-based sorbents for CO2 capture. *Environmental Science and Technology, 44*(24), 9496-9501.

[7] Solieman, A. A. A., Dijkstra, J. W., Haije, W. G., Cobden, P. D., & van den Brink, R. W. (2009). Calcium oxide for CO2 capture: Operational window and efficiency penalty in sorption-enhanced steam methane reforming. *International Journal of Greenhouse Gas Control, 3*(4), 393-400.

[8] Cobden, P. D., Elzinga, G. D., Booneveld, S., Dijkstra, J. W., Jansen, D., & van den Brink, R. W. (2009). Sorption-enhanced steam-methane reforming: CaO-CaCO3 capture technology. Paper presented at the *Energy Procedia, , 1*(1) 733-739.

[9] Elzinga, G. D., Reijers, H. T. J., Cobden, P. D., Haije, W. G., & Van Den Brink, R. W. (2011). CaO sorbent stabilisation for CO2 capture applications. Paper presented at the *Energy Procedia, , 4* 844-851.

[10] Manovic, V., & Anthony, E. J. (2010). CO2 carrying behavior of calcium aluminate pellets under high-temperature/high-CO2 concentration calcination conditions. *Industrial and Engineering Chemistry Research, 49*(15), 6916-6922.
[11] González, B., Blamey, J., McBride-Wright, M., Carter, N., Dugwell, D., Fennell, P., et al. (2011). Calcium looping for CO2 capture: Sorbent enhancement through doping. Paper presented at the *Energy Procedia, , 4* 402-409.
[12] Florin, N. H., Blamey, J., & Fennell, P. S. (2010). Synthetic CaO-based sorbent for CO2 capture from large-point sources. *Energy and Fuels, 24*(8), 4598-4604.
[13] Luo, C., Zheng, Y., Ding, N., Wu, Q., Bian, G., & Zheng, C. (2010). Development and performance of CaO/La2O3 sorbents during calcium looping cycles for CO2 capture. *Industrial and Engineering Chemistry Research, 49*(22), 11778-11784.
[14] Pacciani, R., Müller, C. R., Davidson, J. F., Dennis, J. S., & Hayhurst, A. N. (2009). The performance of a novel synthetic ca-based solid sorbent suitable for the removal of CO2 and SO2 from flue gases in a fluidised bed. Paper presented at the *Proceedings of the 20th International Conference on Fluidized Bed Combustion,* 972-978.
[15] Sultan, D. S., Müller, C. R., & Dennis, J. S. (2010). Capture of CO2 using sorbents of calcium magnesium acetate (CMA). *Energy and Fuels, 24*(6), 3687-3697.
[16] Belova, A. G., & Yegulalp, T. M. (2010). Capture of CO2 from coal gasification gases on a calcium oxide based sorbent. Paper presented at the *SME Annual Meeting and Exhibit 2010,* 318-320.
[17] He, L., Zhao, T., Sultana, S. K., Magnus, R. A., & Chen, D. E. (2010). Progresses in carbonate looping process: Materials and applications. Paper presented at the *ACS National Meeting Book of Abstracts*
[18] Huang, C. -., Chang, K. -., Yu, C. -., Chiang, P. -., & Wang, C. -. (2010). Development of high-temperature CO2 sorbents made of CaO-based mesoporous silica. *Chemical Engineering Journal, 161*(1-2), 129-135.
[19] Li, L., King, D. L., Nie, Z., Li, X. S., & Howard, C. (2010). MgAl2O4 spinel-stabilized calcium oxide absorbents with improved durability for high-temperature CO2 capture. *Energy and Fuels, 24*(6), 3698-3703.
[20] Martavaltzi, C. S., & Lemonidou, A. A. (2010). Hydrogen production via sorption enhanced reforming of methane: Development of a novel hybrid material-reforming catalyst and CO2 sorbent. *Chemical Engineering Science, 65*(14), 4134-4140.
[21] Manovic, V., & Anthony, E. J. (2010). Competition of sulphation and carbonation reactions during looping cycles for CO2 capture by cao-based sorbents. *Journal of Physical Chemistry A, 114*(11), 3997-4002.
[22] Yan, C. -., Chen, Y., Grace, J. R., & Lim, J. (2007). Effects of rapid limestone calcination on carbonation or sulphation of calcined lime by CO2 or SO2. *Ranshao Kexue Yu Jishu/Journal of Combustion Science and Technology, 13*(1), 29-34.
[23] Dobner, S., Sterns, L., Graff, R.A., Squires, A. M. (1977). Cyclic calcination and re-carbonation of calcined dolomite. Industrial & engineering chemistry process design and development, 16(4), 479-486.
[24] Meyer, J., Mastin, J., Bjørnebøle, T. -., Ryberg, T., & Eldrup, N. (2011). Techno-economical study of the zero emission gas power concept. Paper presented at the *Energy Procedia, , 4* 1949-1956.
[25] Cobden, P. D., van Beurden, P., Reijers, H. T. J., Elzinga, G. D., Kluiters, S. C. A., Dijkstra, J. W., et al. (2007). Sorption-enhanced hydrogen production for pre-combustion CO2 capture: Thermodynamic analysis and experimental results. *International Journal of Greenhouse Gas Control, 1*(2), 170-179.
[26] Romano, M. C., Cassotti, E. N., Chiesa, P., Meyer, J., & Mastin, J. (2011). Application of the sorption enhanced-steam reforming process in combined cycle-based power plants. Paper presented at the *Energy Procedia, , 4* 1125-1132.
[27] Elzinga, G. D., Cobden, P. D. & Van Den Brink, R. W. *Unpublished Results*

[28] Harrison, D. P. (2008). Sorption-enhanced hydrogen production: A review. *Industrial and Engineering Chemistry Research, 47*(17), 6486-6501.
[29] Blamey, J., Anthony, E. J., Wang, J., & Fennell, P. S. (2010). The calcium looping cycle for large-scale CO2 capture. *Progress in Energy and Combustion Science, 36*(2), 260-279.
[30] Duan, Y. (2010). Theoretical screening good sorbents for CO2 separation: Application to alkali and alkaline-earth oxides and hydroxides. Paper presented at the *AIChE Annual Meeting, Conference Proceedings*
[31] Fagerlund, J., Nduagu, E., Romão, I., & Zevenhoven, R. (2010). A stepwise process for carbon dioxide sequestration using magnesium silicates. *Frontiers of Chemical Engineering in China, 4*(2), 133-141.
[32] Fricker, K. J., & Alissa Park, A. -. (2010). Enhanced hydrogen production with integrated carbon sequestration using mg(OH)2 sorbent. Paper presented at the *10AIChE - 2010 AIChE Annual Meeting, Conference Proceeding*
[33] Li, B., Wen, X., Zhao, N., Wang, X. -., Wei, W., Sun, Y. -., et al. (2010). Preparation of high stability MgO-ZrO2 solid base and its high temperature CO2 capture properties. *Ranliao Huaxue Xuebao/Journal of Fuel Chemistry and Technology, 38*(4), 473-477.
[34] Wang, Q., Tay, H. H., Ng, D. J. W., Chen, L., Liu, Y., Chang, J., et al. (2010). The effect of trivalent cations on the performance of mg-M-CO3 layered double hydroxides for high-temperature CO2 capture. *ChemSusChem, 3*(8), 965-973.
[35] Inoue, R., Ueda, S., Wakuta, K., Sasaki, K., & Ariyama, T. (2010). Thermodynamic consideration on the absorption properties of carbon dioxide to basic oxide. *ISIJ International, 50*(11), 1532-1538.
[36] Reijers, H., Elzinga, G. D., Cobden, P. D., Haije, W. G., & van den Brink, R. W. (2011). Tandem bed configuration for sorption-enhanced steam reforming of methane. *International Journal of Greenhouse Gas Control, 5*(3), 531-537.
[37] Kim, J. H., Lee, S., Lee, K. S., & Kim, D. K. (2004). The effect of grain boundary phase on contact damage resistance of alumina ceramics. *Journal of Materials Science, 39*(23), 7023-7030.
[38] Blamey, J., Lu, D. Y., Fennell, P. S., & Anthony, E. J. (2011). Reactivation of CaO-based sorbents for CO2 capture: Mechanism for the carbonation of ca(OH)2. *Industrial and Engineering Chemistry Research, 50*(17), 10329-10334.
[39] Domenichini, R., Arienti, S., Cotone, P., & Santos, S. (2011). Evaluation and analysis of water usage and loss of power in plants with CO2 capture. Paper presented at the *Energy Procedia, , 4* 1925-1932.

3.2 CaO and Mg promoted CaO as post combustion CO_2 capture materials

Anne Mette Frey, Dagmar Tulner, Krijn de Jong and Harry Bitter, Utrecht University

3.2.1 Goal

The goal of this study is to evaluate bulk high surface area CaO and MgO-CaO materials for CO_2 capture and to investigate the impact and role of the magnesium.

The materials were prepared by sol-gel synthesis. The influence of synthesis parameters such as water evaporation temperature, metal nitrate to citrate ratio, drying temperature, calcination temperature, heating rate and time were varied in order to obtain an optimal high surface area.

3.2.2 Material prepared by sol gel methods:

5.00 g $Ca(NO_3)_2.4H_2O$ (+or 0.42 g or 0.85 g $Mg(NO_3)_2.6H_2O$) for respectively 5 and 10 wt% Mg containing sample) was dissolved in 25 ml water to which 4.50 g citric acid dissolved in 15 ml water was added (250 ml beaker). The temperature was adjusted to 80 °C while stirring and kept at that temperature until a pale yellow gel was formed. Next the gel was dried in an oven at 135 °C in static air in the beaker for 15 h whereby an intensely colored yellow foam with a volume of around 150 ml was formed. The foam was crushed and heat treated in static air at 850 °C (2 °C/min) for 5 h. The resulting white product, 1.16 g, 20 ml for CaO, 1.24 g, 35 ml for the 10wt% MgO-CaO sample and 1.16 g for the 5 wt% MgO-CaO sample[1].

The sol-gel method is summarized in the scheme below:

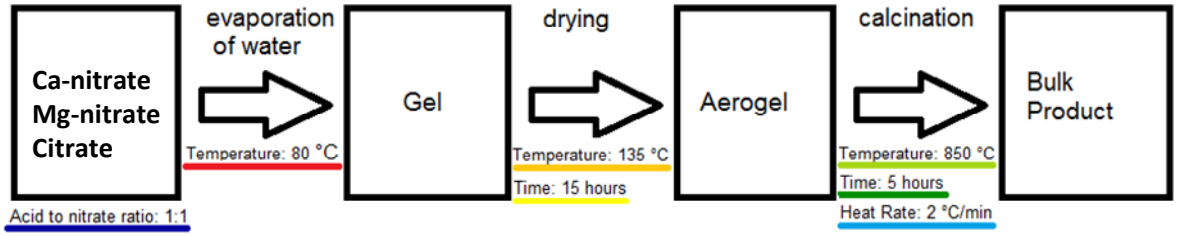

Characterization

Specific surface area:

N_2 physisorption was used to determine the specific surface area, SSA, of the bulk CaO and the Mg containing CaO samples. The standard preparation method described above resulted in a SSA of 10 m^2/g for CaO and 15 m^2/g for 5% Mg CaO. This was reproduced finding respectively 11 and 15 m^2/g for the reproduced sample. Since literature[1] claims that it is possible with this method to obtain SSA of CaO ~40 m^2/g different parameters i.e. the evaporation temperature of the water to form the gel, the drying temperature, the calcination temperature, rate and time were

varied with the expectation that theexpectation that the surface area increased. The SSA's of the CaO and 5% Mg in CaO obtained this way are displayed in Table 1. The standard synthesis described in detail in the experimental is marked with a grey color bar and can thus be compared to the samples where one of the parameters are changed as described in the colored text above the values in the table.

Table 1: *Specific surface area of CaO and 5% Mg containg CaO prepared in different ways. The gray bar indicates the standard synthesis method. This sample is compared to materials where one synthesis parameter (as indicated with the color bars) has been changed.*

		BET surface area m^2/g				BET surface area m^2/g	
evaporation temperature		CaO	CaO 5 wt% MgO	calcination temperature		CaO	CaO 5 wt% MgO
60 ° C	**1a**	16	14	800 ° C	**3a**	19	18
80 ° C	**4b**	10	15	850 ° C	**4b**	10	15
100 ° C	**1c**	13	17	900 ° C	**3b**	16	15
drying temperature				1000 ° C	**3c**	11	13
100 ° C	**2a**	17	21	calcination time			
130 ° C	**4b**	10	15	1 hour	**4a**	16	13
150 ° C	**2c**	16	20	5 hours	**4b**	10	15
drying time				Reproduced 5 hours	**4b REP**	11	15
5 hours	**7a**	15	21	10 hours	**4c**	6	9
10 hours	**7b**	15	21	heat rate calcination			
15 hours	**4b**	10	15	1 ° C / min	**5a**	18	16
20 hours	**7c**	13	19	2 ° C / min	**4b**	10	15
				5 ° C / min	**5c**	17	18
				acid to nitrate ratio			
				1 to 1	**4b**	10	15
				2 to 1	**6c**	16	16

As seen from the screening in the table it is very difficult to draw definite conclusion of the impact of a given parameter. The trends for the CaO and the 5% Mg in CaO are furthermore not the same. However, a few indications about the optimal synthesis route can be deducted: low calcination temperature (800 °C) and short calcination time (most likely between 1 and 5 h) seems to be beneficial for obtaining high SSA products. By keeping the calcination temperature at around 800 °C SSA ~ 20 m^2/g can be obtained for CaO thus a factor 2 higher than the initial sol-gel synthesis attempt. In order to gain insight in the location of the Mg in the Mg containing CaO samples the samples were characterized by XRD and TEM.

3.2.3 XRD and Rietveld analysis

Here the XRD of 10% Mg in CaO prepared by sol-gel method is shown in Figure 2 as an example.

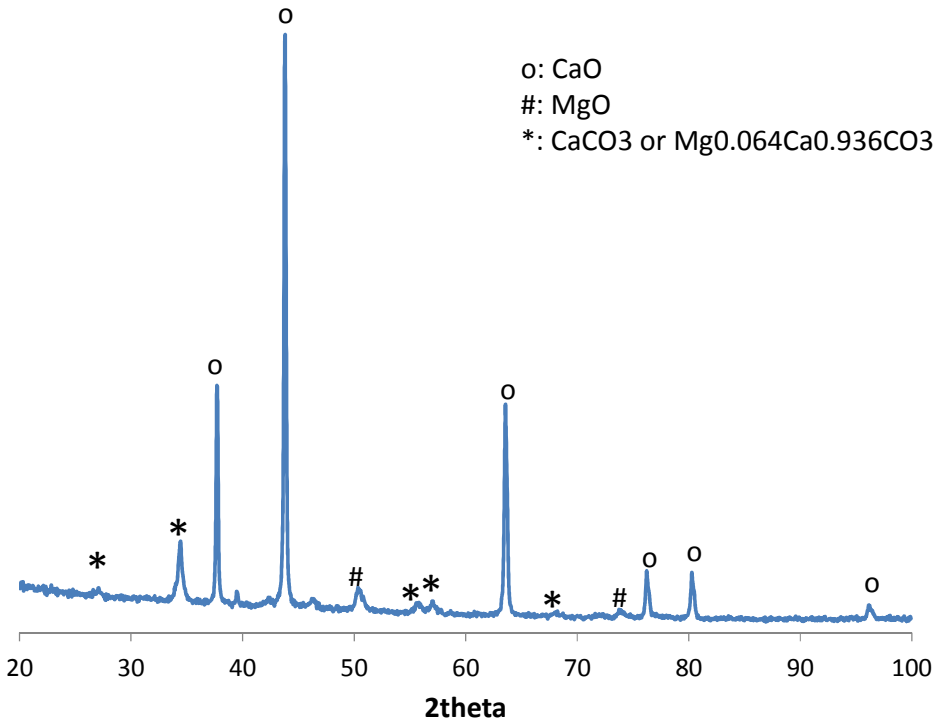

Figure 2. *XRD of 10% Mg in CaO*

As can be seen in Figure 2 the most dominant crystalline phase in XRD is originating from CaO. Furthermore peaks originating from MgO are observed. A third phase can either be assigned to $CaCO_3$ or $Mg_{0.064}Ca_{0.936}(CO_3)$. Rietveld analysis was applied and the weight percentages of the three phases are shown below:

Phase	Weight percentage of the Phase
CaO	68.97
MgO	9.27
$CaCO_3$/ $Mg_{0.064}Ca_{0.936}(CO_3)$	21.77

This analysis clearly shows that most of the magnesium is present as MgO. However it is possible that some Mg is present in a mixed Ca/Mg carbonate. Based on XRD it can

thus neither be confirmed nor excluded that some Mg and Ca are interacting closely in a mixed compound.

3.2.4 TEM analysis

Bright field TEM showed that the sol gel prepared samples consisted of 50-100 nm semi spherical particles clustered together in large particles. In no cases separated particles were observed. In order to gain insight in the location of magnesium line profile EDX experiments were carried out. In Figure 3 an example of a dark field TEM image can be seen (right). The red line indicates where the line profile was intended measured. Due to the long measurement time the sample do, however, move slightly as can be seen by the small holes in the sample (in a curve in the blue box) originating from beam damage by the mapping thus showing the true points measured along a curve deriving slightly from the red line.

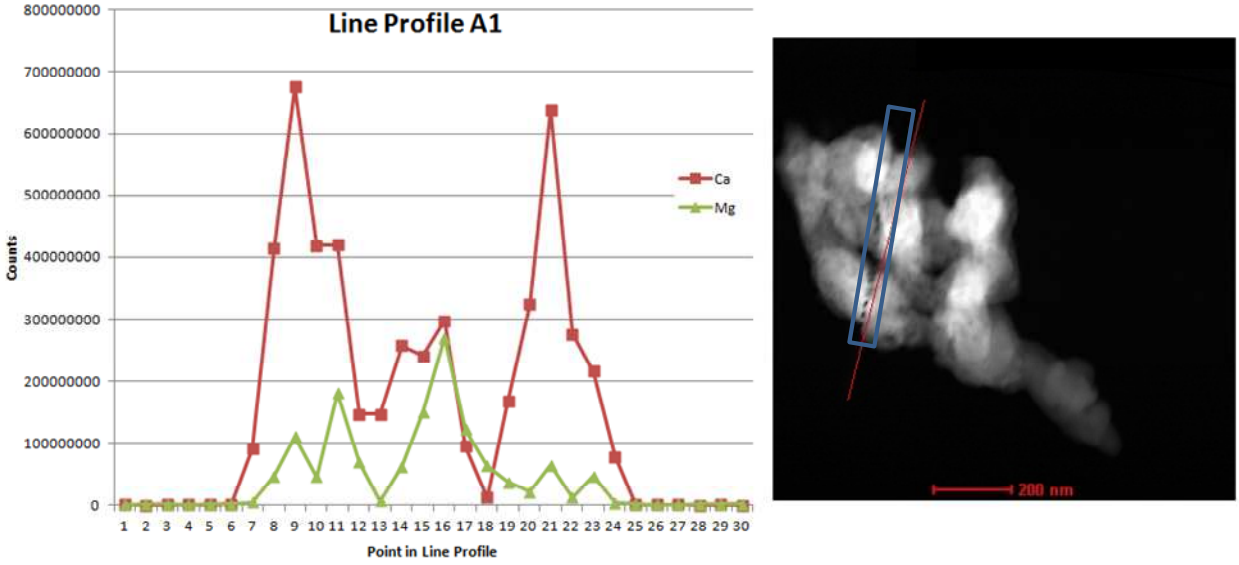

Figure 3. *Line profile (left) and dark field (right) TEM images of 10MgO-CaO*

In the line profile (Figure 3, left) the intensity for the EDX signal of respectively Ca and Mg are shown. The line profile measured moves along 3 of the semi-spherical particles clustered together and it is clear that all three of these particles contain both calcium and magnesium. The ratio between magnesium and calcium varies however significantly, meaning that the magnesium is not homogeneous distributed in the sample at this nm scale. This is in accordance with the observation in XRD of a separate MgO phase. However, on the other hand the line profile (along with a number of other line profiles of the sample) clearly shows that the MgO and CaO phases must be in proximity of each other since no distant single particles were found.

3.2.5 DFT

A theoretical way to gain insight in the role of Mg as promotor for CO_2 capture in CaO could be using DFT calculations. It might be possible to calculate if there is a stabilization energy effect for small particles (thus avoiding sintering) by having Mg in a CaO structure, or by having small MgO particles in the proximity of CaO particles. Furthermore adsorption energies of CO_2 on respectively CaO, MgO and sites close to both metals could be calculated and compared. Initial calculations of adsorption of CO_2 on MgO and CaO surfaces have been performed. The adsorption of CO_2 on MgO is shown in Figure 4.

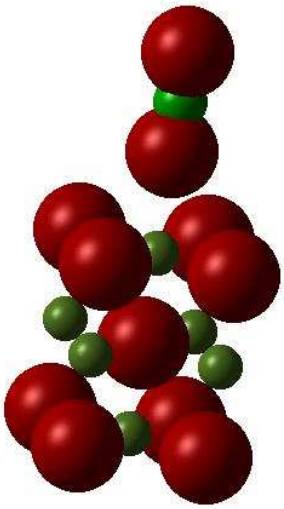

Figure 4: *CO_2 adsorption on MgO, calculated using CRYSTAL*

The conclusion of this preliminary study is however that this will be too complicated to study systematically in the remaining time of the project - unless a collaboration with a research group specialized in these kind of problems and calculations would be possible.

3.2.6 Performance of the materials for CO_2 capture

The performance for CO_2 capture of the sol gel prepared standard sample CaO and 5% Mg in CaO were investigated and compared to a commercial available high surface area CaO sample (40 m^2/g). Temperature programmed desorption of CO_2 was used to evaluate CO_2 capture properties. All three samples were activated in the TPD apparatus by heat treatment to 800 °C in He. It should be noted that this pretreatment procedure resulted in a significant decrease in specific surface are of the commercial CaO sample to 9 m^2/g. After the heat treatment the samples were cooled down to 40 °C where CO_2 was pulsed over the sample until saturation. After the CO_2 pulses the samples were heated in He to 800 °C (10 °C/min) and TPD was performed. Next the sample was cooled to 40 °C and new CO_2 pulse/desorption cycle were performed twice. The results

are compiled in Figure 5. A peak in the TPD figure at 600 °C is dominant for all three samples. This signal is representative for the decomposition of $CaCO_3$.

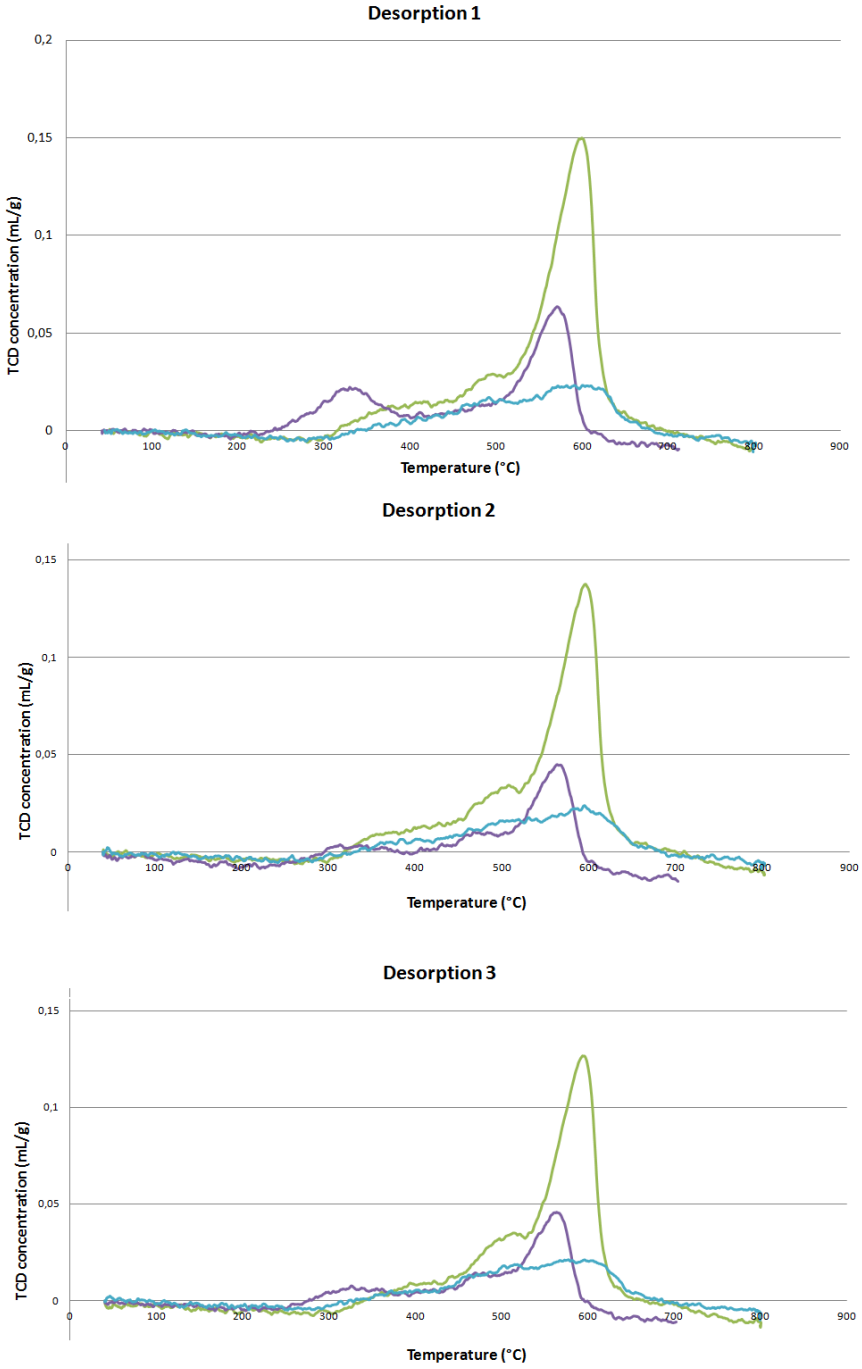

Figure 5. *Temperature programmed desorption of CO_2 in three recycles of: Green commercial CaO, purple sol gel prepared CaO, blue sol gel prepared 5% Mg-CaO.*

It is however noteworthy to mention that there is a distinct peak at 300 °C for the sol gel prepared CaO sample (most clear in the first desorption). Thus a part of the CO_2 must be weaker bounded to CaO.

For the Mg containing sample a very broad desorption peak is always observed.
The values for the total CO_2 uptake and release in the three cycles can be seen in Table 2 (the three samples in the top of the table). The theoretical max value for the CO_2 uptake is calculated to 399 ml/g CaO.

Table 2. *Adsorption and desorption of CO_2 in different CaO materials*

Sample	adsorption 1 (mL/ g STP)	desorption 1 (mL/ g STP)	adsorption 2 (mL/ g STP)	desorption 2 (mL/ g STP)	adsorption 3 (mL/ g STP)	desorption 3 (mL/ g STP)
Comm CaO	8.0	3.6	4.5	3.6	4.8	3.3
Sol gel CaO	2.7	1.5	2.0	1.2	1.8	1.1
5% Mg solg CaO	2.7	2.2	2.3	2.0	2.5	2.0
Ca(OH)2	4.0	3.5	3.8	3.1	3.6	3.1
MgO/CaO	1.2	1.2	0.8	0.9	0.8	0.8

It can be concluded that for all materials less than 1% of the CO_2 capacity is used. In the following we will consider the CO_2 capacity and stability of the materials closer.

For the heat treated commercial CaO sample the desorption (3.6 ml/g) is much less that the CO_2 adsorped (8.0 ml/g) in the first cycle. This indicates that not all CO_2 is desorbed from the sample. In the following cycle only 4.5 ml/g is taken up which matches well with the fact that the capacity is lowered by some CO_2 being bound irreversible. The CO_2 uptake decreased 40% from the first to the third cycle for the commercial CaO sample. The two sol gel prepared CaO samples, with and without Mg, showed similar CO_2 uptake in the first cycle. Though this uptake, 2.7 ml/g, was smaller than for the commercial CaO sample, the materials seemed more stable in the recycling. The CO_2 uptake for the sol gel prepared CaO sample decreased 33% from the first to the third cycle while the MgO containing CaO sample decreased only 7%. It should be noted that for all three samples the majority of the change in CO_2 capacity take place between the first to the second cycle, and all samples seems relatively stable between the second and the third cycle. If looking at the difference between adsorption and desorption for the sol gel prepared sample it is clear that the Mg containing sample is performing better. In the first run 80% of the adsorped CO_2 is desorped while only 55% of the CO_2 is desorped from the CaO sample.

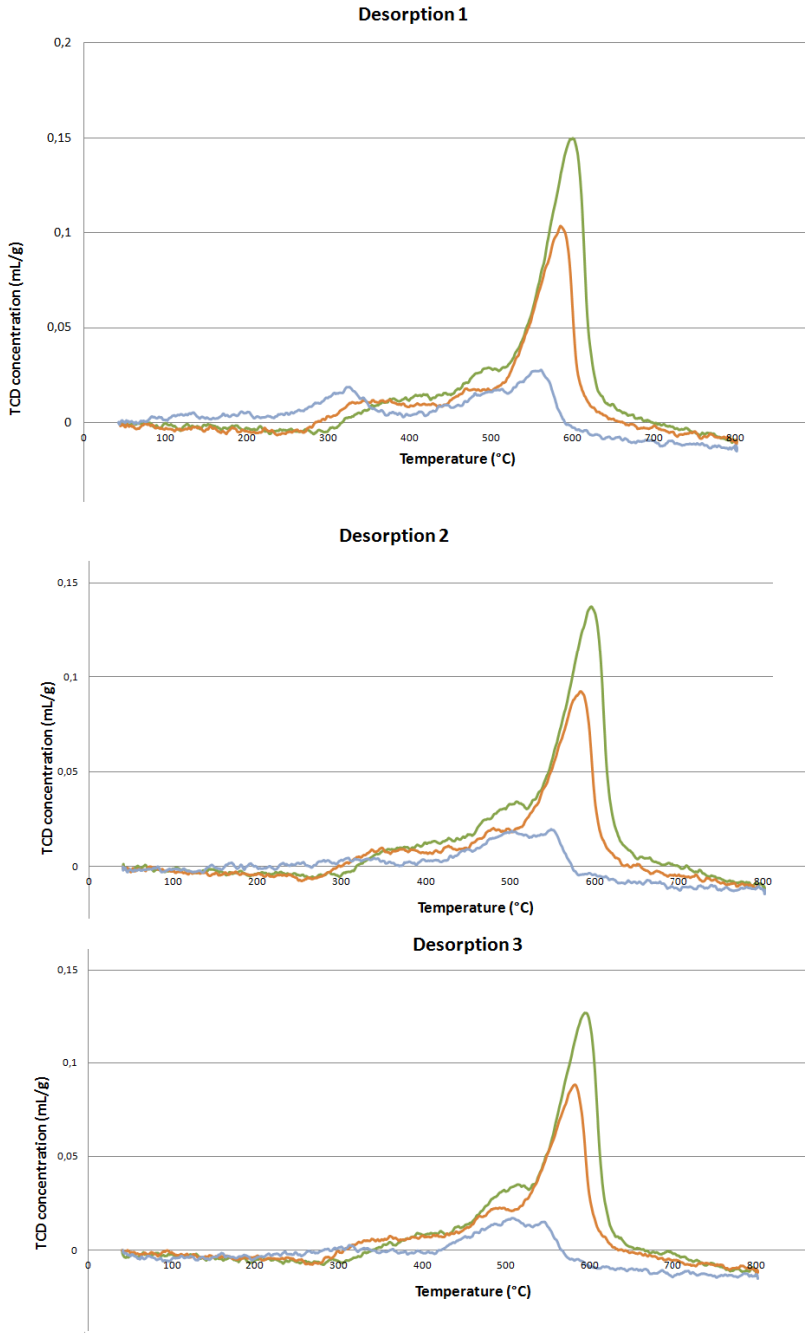

Figure 7. *CO_2 TPD in three recycles of: Green commercial CaO, orange commercial CO_2 treated with water before test, blue 5% Mg impregnated on commercial CaO.*

Since Mg promotion seems to the material easier regenerable and increased the stability of the CaO as CO_2 capture material for the sol gel prepared samples, we investigated the impact of magnesium in other CaO materials. Another material was prepared by introducing magnesium to the commercial CaO. This was prepared by incipient wetness impregnation of magnesium nitrate in water, followed by drying and calcination (5 wt% MgO). Since water can interact with CaO (to form $Ca(OH)_2$) an additional sample, '$Ca(OH)_2$', was prepared by impregnating CaO with water, drying and heat treating it. This way it could be investigated if the water could damage the CaO material and thereby influenced the CO_2 capture performance.

In Figure 6 the three CO_2 TPD cycles are shown for these two samples (MgO/CaO and '$Ca(OH)_2$') after heat treatment to 800 °C together with the data for the commercial CaO for comparison. The adsorption/desorption values are reported in the lower part of Table 2. It is clear that the CaO and $Ca(OH)_2$ samples have a comparable TPD profile. The MgO/CaO sample does, however, behave very differently. Again, as it was also seen for the Mg CaO sol gel sample, the TPD peak has become very broad. For the impregnated sample the total amount of adsorped CO_2 is much less, 1.2 ml/g than for the parent commercial CaO sample, 8.0 ml/g (or for the sol gel samples discussed above 2.7 ml/g). Though the CO_2 capacity is low all CO_2 adsorped on the MgO/CaO sample is desorbed again in the first cycle. However, the CO_2 capacity decreases tremendously when evaluating the adsorption from 1. to 3. cycle, with 33% for MgO/CaO. Due to the performance of the $Ca(OH)_2$ sample it could be ruled out that differences between CaO commercial and MgO/CaO was due to the $Ca(OH)_2$ phase formed by impregnation and the possibly non-reversibility to CaO without e.g. surface area damaged. The changed properties can thus be ascribed to the presence of magnesium in the sample.

Thus magnesium seems to have a promising effect for stability and the possibility for regeneration in the sol gel method, but when impregnating it to commercial CaO it has no stabilizing effect. The location of Mg must thus be considered crucial for the impact on the performance of CaO CO_2 capture materials.

3.2.7 References

[1] E.T. Santos et al, Fuel 94 (2012) 624-628

3.3 Calcium oxide supported on zirconia as CO_2 capture materials

Anne Mette Frey, Krijn P. de Jong and Johannes Hendrik Bitter

3.3.1 Introduction and aim

Previous studied has shown that bulk CaO has low CO_2 capture capacity. Our preliminary fundamental studies have shown that nano-sizing CaO and stabilizing it on an inert carbon support increases the capacity. However, for industrial post combustion application a carbon support is not suitable, since it is not stable with respect to steam at high temperature. Other supports must thus be considered. In this study we have performed a screening of several oxidic supports showing that zirconia is a promising candidate. The calcium oxide-zirconia system has thus been studied in more detail to obtain further knowledge of the possibility of using the material as a solid CO_2 capture material. For CaO-loaded zirconia a capture capacity of 0.4-0.5 mmol/g (sorbent basis) has been found; desorption of CO_2 typically takes place in the temperature range of 625-800 °C.

3.3.2 Preparation of materials

Chemicals:

Magnesium nitrate hexahydrate (99+%) was obtained from Acros and acetone (HPLC grade) was obtained from Fluka. Calcium nitrate tetrahydrate (99%), strontium nitrate (p.a.), barium nitrate, iso octane (99%) and $ZrO(NO_3)_2.2H_2O$ (99%) were obtained from Sigma-Aldrich.

Support materials

γ-Al_2O_3 (Engelhard), ZrO_2 (Degussa), α-Al_2O_3 (BASF), oxidized carbon nanofibers, CNF. The CNFs were prepared as follows: A 5% Ni/SiO_2 catalyst was prepared by deposition precipitation synthesis at 90 °C, using nickel nitrate hexahydrate (7.72 g), SiO_2 (25.5 g, Aerosol 300, Degussa) and urea (27.7) in 1 l of water. This material was used as growth catalyst after calcination (600 °C) and reduction (700 °C). Carbon nanofibers were grown

from 5 g of the growth catalyst using syngas (H_2/CO/N_2 102/266/450 ml/min) at 550 °C and 3.8 bars pressure. The fibers were purified by a treatment in refluxing 1 M KOH (1.5 h) to remove the silica and a subsequent treatment, after washing, in refluxing concentrated HNO_3 (1.5 h) to remove nickel and to functionalize the fibers. 30 g of oxidized carbon nanofibers was typically obtained after the washing of the material.

5 and 10 wt% CaO introduced to different supports by impregnation:

CaO/ZrO_2: The zirconia was dried in static air for 2 h at 120 °C. 2.5 g of the dried ZrO_2, denoted s-ZrO_2, (pore volume of 0.68 ml/g) was placed in a 50 ml impregnation flask under vacuum for 30 minutes. Calcium nitrate was introduced by incipient wetness impregnation using 1.7 ml 1.93 M solution of an aqueous $Ca(NO_3)_2.4H_2O$ solution. The sample was allowed to equilibrate for 1 h, followed by drying at 120 °C for 12 h in static air. This resulted in 5wt% CaO/ZrO_2. A second impregnation step was performed in order to obtain 10 wt% loading.

The materials were crushed and sieved to particles of 25-150 micron. The samples were heat treated in 30 ml.min^{-1} N_2 as standard at 600 °C (800 °C in specific cases) for 3 h (5 °C.min^{-1}) immediately prior to the catalytic test.

CaO on the other supports were prepared following the same procedure and will be named CaO/support

Alkaline earth metal oxide supported on zirconia

The same procedure as for CaO/ZrO_2 mentioned above was applied: 3.4 wt% MgO, 5.0 wt% CaO, 8.8 wt% SrO and 13 wt% BaO (same molar amount of the alkaline earth metal ion) was introduced to ZrO_2 by incipient wetness impregnation using aqueous solutions of the metal nitrates. In the case of the BaO sample five impregnations with barium nitrate were needed to obtain the required loading. After impregnation the samples were equilibrated for 1 h followed by drying in stagnant air for 12 h at 120 °C. The samples were activated as described for CaO/ZrO_2.

Precipitation

Co-precipitation of CaO-ZrO_2 (containing 5% CaO) was performed as follows: 7.00 g $ZrO(NO_3)_2.2H_2O$ and 0.72 g $Ca(NO_3)_2.4H_2O$ was dissolved in 100 ml of water. This solution was added drop wise to 50 ml of water in a double walled thermostatted batch glass reactor at 40 °C in which the pH had been adjusted to 10 by adding a few drops of an ammonia solution. While adding the metal salt solution (duration 30 minutes) the pH was kept constant at 10 by adding a 2.8 M NH_3 solution drop wise while stirring vigorous. After 4 h of precipitation and ageing at 40 °C the formed, white precipitate was isolated by centrifugation and washed with 3 x 50 ml of water. The sample was died over night at 120 °C and the next day 2.8 g (85 % yield) of pale orange product could be collected.

A sample of ZrO_2 precipitated without calcium was synthesized in the same way, just omitting the adding of calcium nitrate in the synthesis. This sample is denominated ZrO_2 precip.

The samples were activated as described for CaO/ZrO_2.

Characterization

N_2-physisorption experiments were performed at -196 °C on a Micrometrics Tristar Surface Area and Porosity analyzer. The measurements were used to determine pore volumes and specific surface areas of the catalysts.

Volumetric CO_2 adsorption was carried out with a Micromeritics ASAP 2010C at 0 °C after drying the samples at 450 °C in vacuum for at least 20 h prior to measurements in the set-up. Prior to the vacuum drying all samples had been heated to 600 °C in nitrogen for 3 h under similar condition as before the catalytic tests. The adsorption measurements were performed by dosing CO_2 measuring the uptake versus the absolute pressure. The total number of basics sites was determined by extrapolation the linear part of the isotherm (100-250 mbar) to zero pressure.

CO_2 TPD was measured on a Micromeritics ASAP 2920 using 100 mg of sample. The samples were pretreated in a heat flow of 30 ml/min He 600 °C for 1 h (5 °C/min). The samples were cooled to 40 °C and CO_2 loaded with pulses of 10% CO_2/He (loop size 0.5311 ml) until saturation. The TPD was performed by heating to 1000 °C with 10°C/min in 30 ml/min He. A second cycle was performed by repeating the CO_2 pulse and the desorption procedure.

The supported samples were examined with transmission electron microscopy (TEM) using an FEI Tecnai 12 or an FEI Technai 20F. The samples were placed on holy carbon grid and both bright field and dark field TEM images were recorded.

SEM micrographs were obtained using a Philips XL30FEG electron microscope equipped with an EDX detector for elemental analysis. The samples were placed on a carbon grid and coated with platinum before measurements to prevent charging.

The XPS measurements are carried out with a Kratos AXIS Ultra spectrometer, equipped with a monochromatic X-ray source and a delay-line detector (DLD). Spectra were obtained using the aluminium anode (Al Kα = 1486.6 eV) operating at 150W. Survey scans were measured at a constant pass energy of 160 eV and region scans at 40 eV. The background pressure was 2 x 10^{-9} mbar.

3.3.3 Results and discussion

Screening of support materials for CO_2 capture materials

In previous work we have reported on carbon nanofibers being an interesting support for solid base CO_2 capture material since the support is inert. This means that CNF cannot form any mixed oxide phase such as it has been suggested for e.g. Al_2O_3 lowering the basicity/availability of base sites and thereby the performance. One issue is however, that carbon supports is not applicable in industrial post combustion applications since it is not stable in the steam at high temperature. Alternatives must thus be considered. In this study we focus on developing supported CaO based CO_2 post combustion material since CaO is widely available, cheap and environmentally benign.

In a screening study 10wt% CaO on different supports (carbon nanofibers (CNF), α- and γ-Al_2O_3, and ZrO_2) prepared by incipient wetness impregnation and activation by heat treatment was compared with bulk CaO as CO_2 capture materials evaluated with CO_2 TPD. The CO_2 desorption profiles are shown in Figure 1.

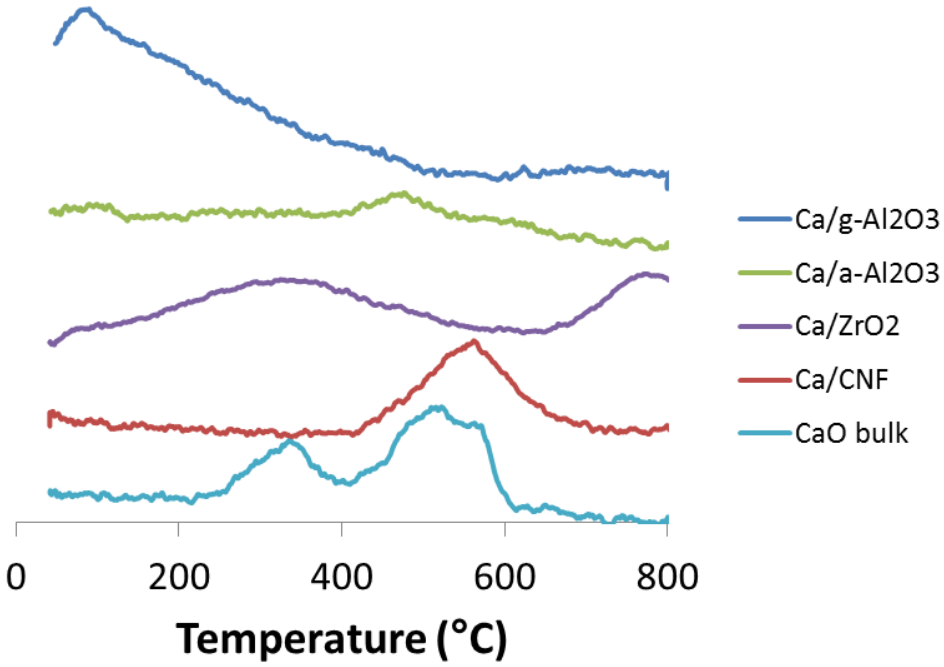

Figure 1. CO_2 desorption profiles for bulk CaO and 10wt% CaO on different supports. The desorption has been normalized per gram sorbent so the intensities of the peaks are directly comparable.

From Figure 1 it is seen that the γ-alumina is desorbing CO_2 at too low temperature for post combustion (~200 °C) and α-alumina is barely showing any CO_2 release at all. This indicates that the two alumina supports are not suitable for post combustion CO_2 capture. CaO on ZrO_2 on the other hand shows two desorption peaks, one at 300 °C and one at higher temperature, 800 °C thus being potentially promising for post-combustion capture. Interesting the desorption peak at 800 °C is located at higher temperature that what is thermodynamic expected (~600 °C). This indicates strong interaction between Ca and ZrO_2 resulting in some very strong base sites. The bulk CaO and CaO/CNF shows CO_2 adsorption at ~600 °C as expected. The CaO/γ-Al_2O_3, CaO/CNF and CaO/ZrO_2 were characterized in order to gain insight in the different behavior between the materials. In Figure 2 the TEM images are shown.

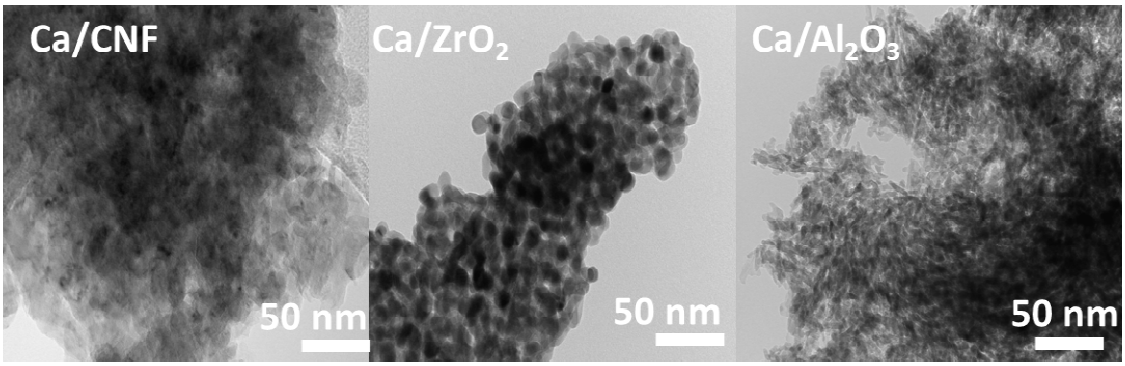

Figure 2 TEM images of CaO/CNF, CaO/ZrO_2 and CaO/Al_2O_3.

The TEM images show that 3 nm CaO particles (well dispersed) are formed on the CNF. For CaO/ZrO_2 and CaO/Al_2O_3 no CaO particles can be observed with TEM. This indicates that the CaO is either very well dispersed i.a. film or is incorporated in the support (i.a. interlayer or solid solution).

The CO_2 uptake determined by chemisorption and the specific surface areas of the materials are reported in the upper part of Table 1.

Table 1 CO_2 uptake and specific surface area of the investigated CO_2 capture materials. All materials have been heat treated at 600 °C unless otherwise stated.

Catalyst	**CO_2 uptake µmol/g**	**Specific surface area m^2/g**
CNF	9	190
CaO/CNF	154	143
Al_2O_3	76	150
CaO/Al_2O_3	419	147
ZrO_2	459	91
CaO/ZrO_2	504	69
CaO/ZrO_2,800°C	423	-
ZrO_2 precip	224	111
$CaO\text{-}ZrO_2$	371	106
MgO/ZrO_2	411	-

SrO/ZrO_2	609	-
BaO/ZrO_2	450	-

It is clear that the CO_2 up-take is very different for the different supported CaO samples. Furthermore it can be noticed that the Al_2O_3 as well as ZrO_2 support themselves contains considerably amount of base sites making the comparison of the sites related to CaO difficult.

Due to the high CO_2 uptake (Table 1) and desorption of CO_2 in an interesting temperature regime when using zirconia as a support (Figure 1), the $CaO\text{-}ZrO_2$ system was investigated in more detail.

Zirconia as a support for CaO

The impact of the preparation method were evaluated by comparing impregnated samples CaO/ZrO_2 and precipitated samples $CaO\text{-}ZrO_2$ (both 5 wt% CaO loading) with the corresponding ZrO_2 support and precipitated ZrO_2.

The specific surface area and number of the base sites were evaluated using respectively BET and CO_2 chemisorption; these results have been summarized in Table 1. The number of base sites is difficult to compare due to the amount of base sites found in zirconia self. It seems, however, to be so that the CaO/ZrO_2 sample (504 µmol/g; ZrO_2 459 µmol/g) has more base sites than the $CaO\text{-}ZrO_2$ (371 µmol/g; ZrO_2 224 µmol/g). The specific surface area is however opposite, larger for $CaO\text{-}ZrO_2$ (106 m^2/g) than for CaO/ZrO_2 (69 m^2/g). The base strengths of CaO/ZrO_2 and $CaO\text{-}ZrO_2$ and thus the temperature at which CO_2 can be released were evaluated using CO_2 TPD as displayed in Figure 3. The results were compared to those found for ZrO_2 support and ZrO_2 precipitated.

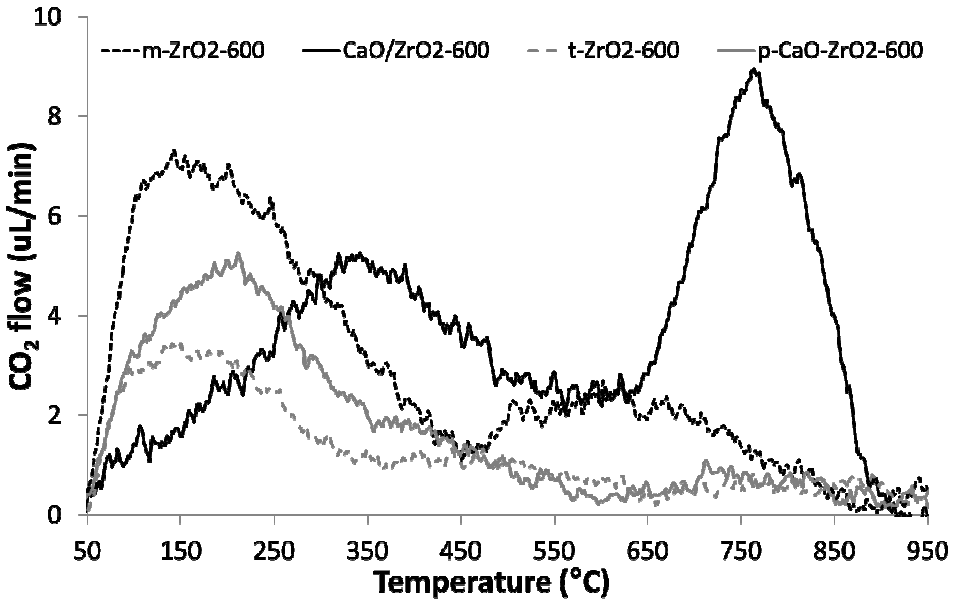

Figure 3 CO_2 TPD CaO/ZrO_2, $CaO\text{-}ZrO_2$, ZrO_2 support and ZrO_2 precipitated

From the CO_2 TPD it can be seen that both zirconia samples (support and precip) display one broad desorption peak at low temperature, with a maximum ~200 °C. This peak can be ascribed to weak basic sites in the intrinsic zirconia surface. For the CaO/ZrO_2 this low temperature peak is shifted to a maximum at 375 °C indicating that the weaker base sites in this sample are stronger sites than in the ZrO_2 support. This suggests that part of the calcium has been dissolved in the structure. At the same time a peak with maximum ~ 775 °C is observed, indicating that the sample contains some very strong base sites most likely associated to the presence of a film/monolayer of CaO on the ZrO_2 surface. For the precipitated $CaO\text{-}ZrO_2$ sample the low temperature peak is also shifted towards higher temperature, 250 °C, but to a less extend that for the impregnated sample which could be explained by part of the calcium sitting in the zirconia lattice structure. A very broad but low intense peak is observed at 600-900 °C for $CaO\text{-}ZrO_2$. The fact that this high temperature peak has so low intensity indicates that only few strong base sites are present, compared to in CaO/ZrO_2. The $CaO\text{-}ZrO_2$ and CaO/ZrO_2 show thus very different properties with respect to the temperature at which

CO_2 is released, dependent on the preparation method and the calcium-support interaction. In order to evaluate this further the samples were characterized in detail.

XRD patterns of the materials were evaluated to gain insight of the structure of the different materials as displayed in Figure 4.

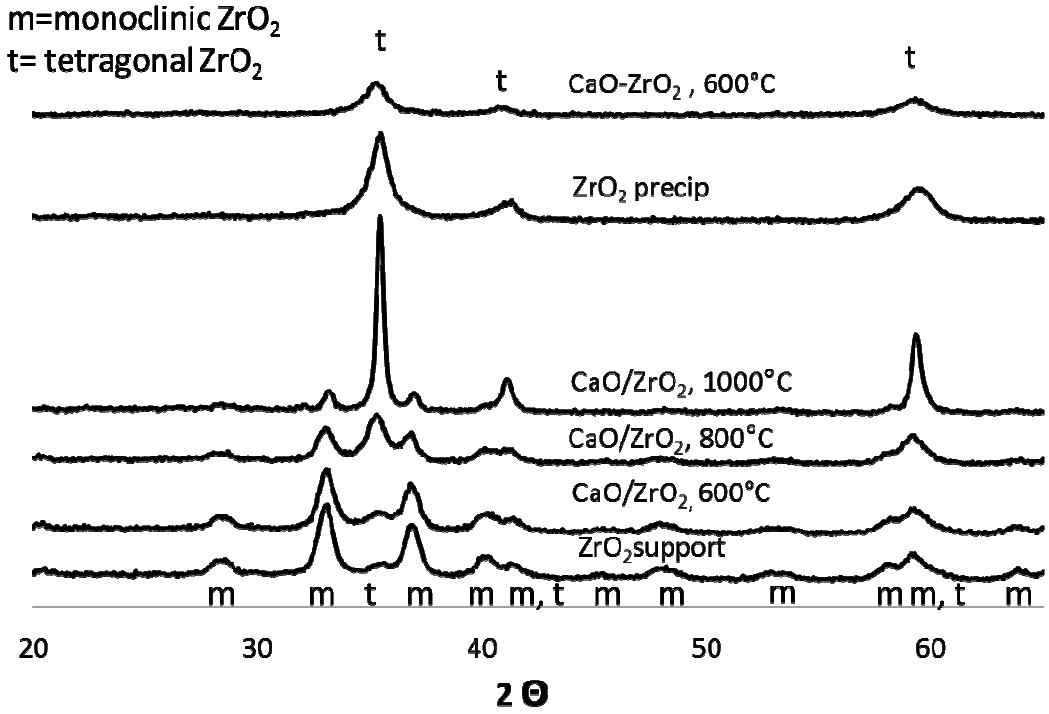

Figure 4. XRD patterns of $CaO\text{-}ZrO_2$ after heat treatment at 600 °C, precipitated ZrO_2 after heat treatment at 600 °C, CaO/ZrO_2 after heat treatment at 600, 800 and 1000 °C, ZrO_2 support.

No peaks originating from CaO is observed in any of the XRD patterns of the materials displayed in Figure 4. The precipitated ZrO_2 and co-precipitated $CaO\text{-}ZrO_2$ shows diffractions from a tetragonal zirconia phase. The impregnated CaO/ZrO_2 and the ZrO_2 support after heat treatment at 600 °C showed diffractions from a monoclinic zirconia phase along with traces of tetragonal zirconia, identified by the low intensity peak at 2Θ =36°. A partial phase transformation of monoclinic zirconia into tetragonal zirconia was observed when heat treating the impregnated sample, CaO/ZrO_2 to 800 °C. When

heating the temperature to higher temperature, 1000 °C the phase transformation is almost total. This means that the material is not stable at high temperature which is a factor that should be considered with respect to applicability and regeneration. The CaO/ZrO_2 and $CaO\text{-}ZrO_2$ was examined with SEM (Figure 5a and 5b respectively) and with TEM (Figure 5c and 5d respectively) to gain insight on the morphology.

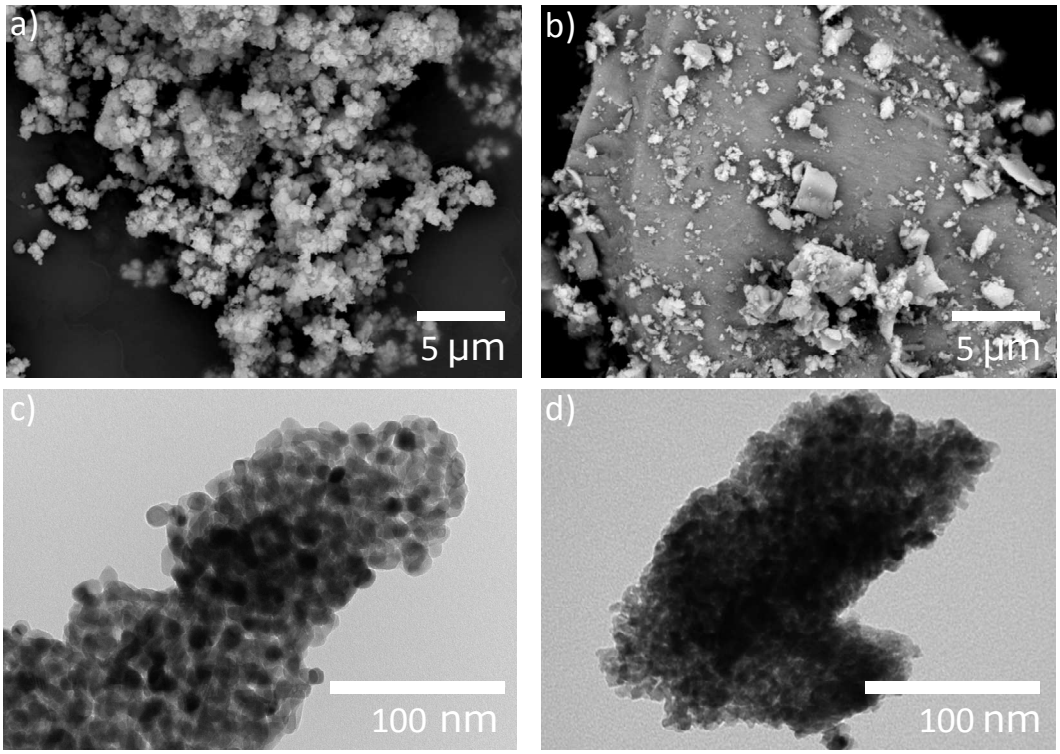

Figure 5 a) SEM of CaO/ZrO_2 b) SEM of $CaO\text{-}ZrO_2$ c) TEM of CaO/ZrO_2 d) TEM of $CaO\text{-}ZrO_2$, all samples have been heat treated at 600 °C

The impregnated CaO/ZrO_2 sample consisted of 1-5 µm lumps, built up from clusters of ~10 nm primary particles (Figure 5a). The precipitated sample $CaO\text{-}ZrO_2$ was more inhomogeneous and consists of both large lumps (~50 µm) with flat surfaces and smaller (1-5 µm) lumps on top. In Figure 5b an example of one such large lump is displayed with smaller parts of the material deposited on the surface. EDX analysis showed that the composition of Zr and Ca is the same for both the large and the small lumps in the precipitated sample. The morphology of ZrO_2 and ZrO_2 precip resembled those of respectively CaO/ZrO_2 and $CaO\text{-}ZrO_2$ (see supplementary material S1). The presence of

calcium was verified with EDX but individual CaO particles were not observed. In TEM the two materials, CaO/ZrO_2 and $CaO\text{-}ZrO_2$ (Figure 5c-d) looked comparable and again the materials were found to be indistinguishable in morphology to zirconia reference samples. In TEM the calcium oxide could thus also not be observed directly but EDX confirmed that for both preparation methods the element ratios correspond to the expected loading of calcium.

In Figure 5 element mapping by SEM of CaO/ZrO_2 is shown. From this it can be seen that the Ca is well distributed over the zirconia within the boundaries of the resolution obtainable with SEM. The same holds true for the co-precipitated sample (see supplementary material S2). This is in accordance with EDX line profile scans in TEM which showed that the calcium and zirconium were always in close proximity. The fact that the calcium cannot be visualized indicated that the CaO is present either in form of a thin film over the surface, as very small particles (< 1 nm), incorporated in the structure of the zirconia or forming a solid solution as suggested in the

literature

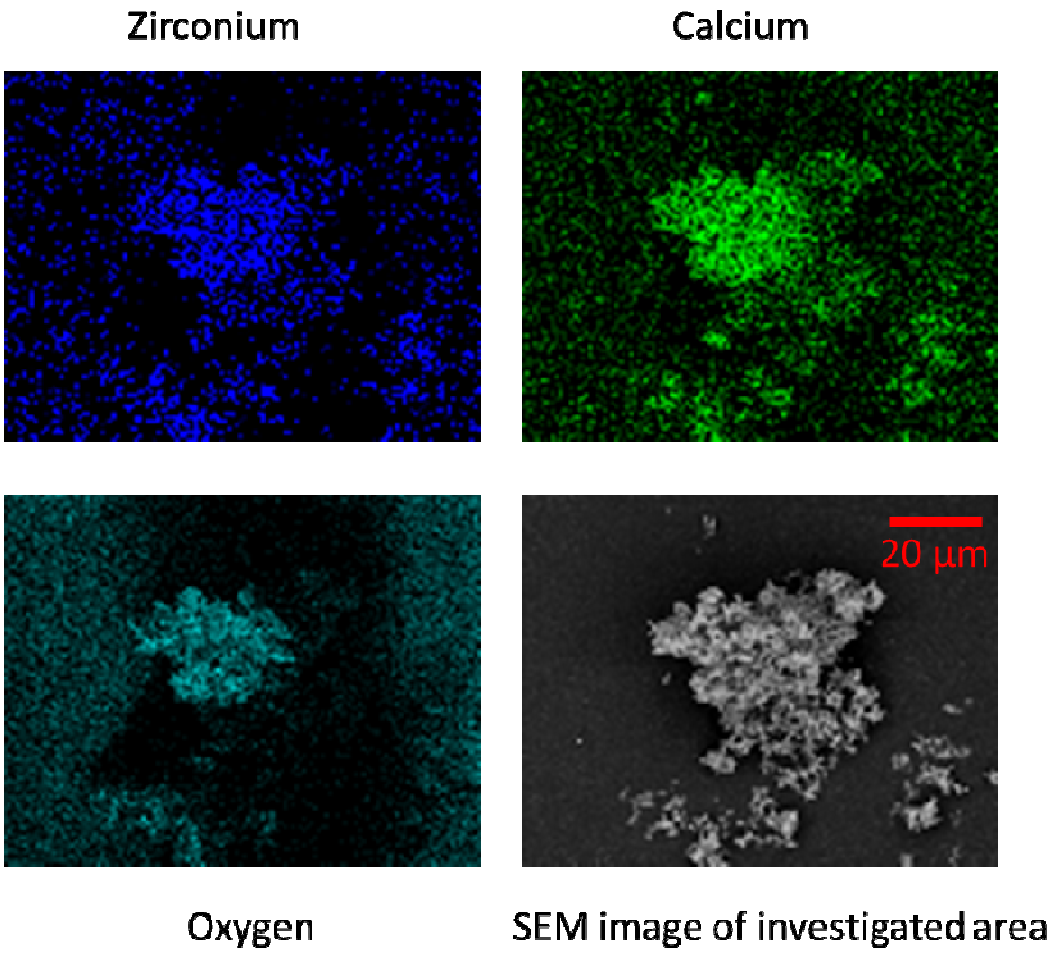

Figure 6 SEM and element mapping of Ca, Zr, O for CaO/ZrO_2

In order to gain more insight in the location of calcium in the two samples XPS was performed. A difference was found between the two samples with CaO/ZrO_2 having 75% surface calcium while $CaO\text{-}ZrO_2$ had only 50%. Since the two samples have the same bulk Ca/Zr composition it is expected that some of the calcium has been incorporated in the structure in the precipitated sample. The higher calcium content in the surface of the impregnated sample might play a role in the higher activity displayed by this sample and suggests that CaO is well dispersed (e.g. film) on the zirconia surface. The XPS results showing more calcium is present on the surface for the impregnated sample than for the

precipitated is consistent with the CO_2 uptake difference for impregnated samples versus precipitated samples.

The CO_2 desorption profiles were evaluated for samples with different CaO loading as seen in Figure 7.

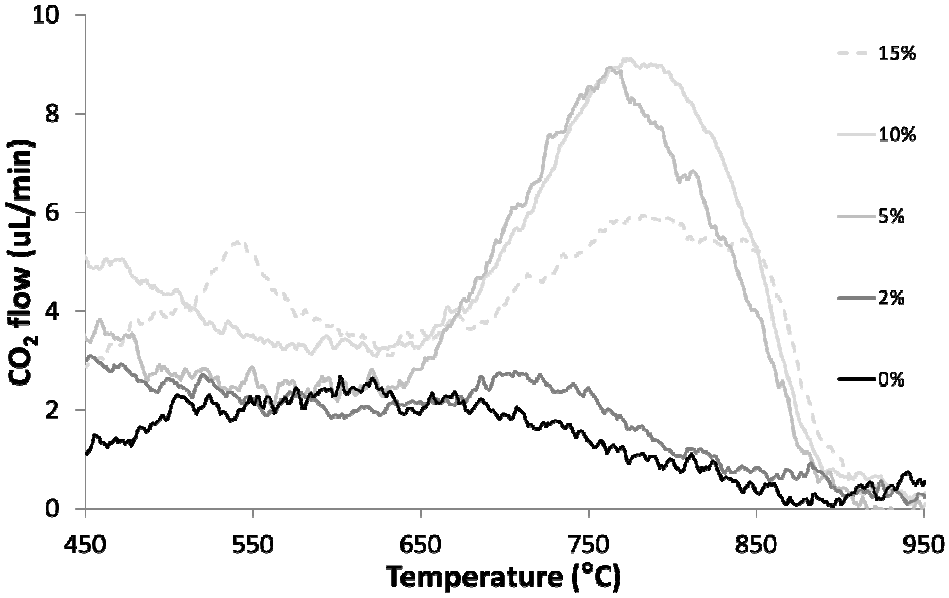

Figure 7. CO_2 desorption versus temperature for CaO/ZrO_2 samples with different loadings (respectively 0, 2, 5, 10, and 15 wt%)

The exact location of the maximum of the peak is shifted by an increase from 725 to 800 °C as the loading is increasing. Qualitatively the height of this peak is following the calcium loading from 0 to 10 wt% CaO. For the 15 wt% sample this peak is decreasing while a more distinguished peak is arising at lower temperature ~540 °C. One monolayer CaO on ZrO_2 support corresponds to 7 wt% CaO but since there are indications (the present of a low temperature CO_2 desorption peak, Figure 3) that some of the CaO is dissolved in the structure it is possible that slightly higher loading i.e. 10 wt% can be deposited on ZrO_2 as monolayer/thin film. For the 15 wt% CaO sample the nature of the sample is clearly different than for the other samples with the additional peak at ~540 °C. The quantitative TPD results are summarized in Table 2 where we distinguish between

low temperature desorption (<450 °C), medium (450-625 °C) and high temperature desorption (>625 °C).

Table 2 Distribution of strong, medium and weak base sites based on CO_2 TPD

Catalyst	**CO_2 release ($\mu mol.g^{-1}$)**			
	Total	**Strong sites (> 625 °C)**	**Medium sites (> 450 °C)**	**Weak sites (< 450 °C)**
ZrO_2 support	115	13	0	102
CaO/ZrO_2	142	63	6	73
CaO/ZrO_2-800	192	25	0	167
2% CaO/ZrO_2	118	17	0	101
10% CaO/ZrO_2	184	68	25	91
15% CaO/ZrO_2	131	41	13	77
ZrO_2 precip	54	7	0	47
$CaO-ZrO_2$	69	9	0	60

It is well-known that the different alkaline earth metal ions have different ionic ratios and thus should show increasing base strength following the trend MgO<CaO<SrO<BaO. This should influence the values of CO_2 desorption temperature in a systematic way for the four metal oxides. We investigated if this was also the case for the metal oxides supported on ZrO_2. Samples containing the same molar loading of alkaline earth metal oxides MgO, CaO, SrO and BaO as in 5 wt% CaO/ZrO_2 was prepared on zirconia by impregnation of the respective nitrates and heat treatment at 600 °C. The desorption profiles of the 4 materials are shown in Figure 8.

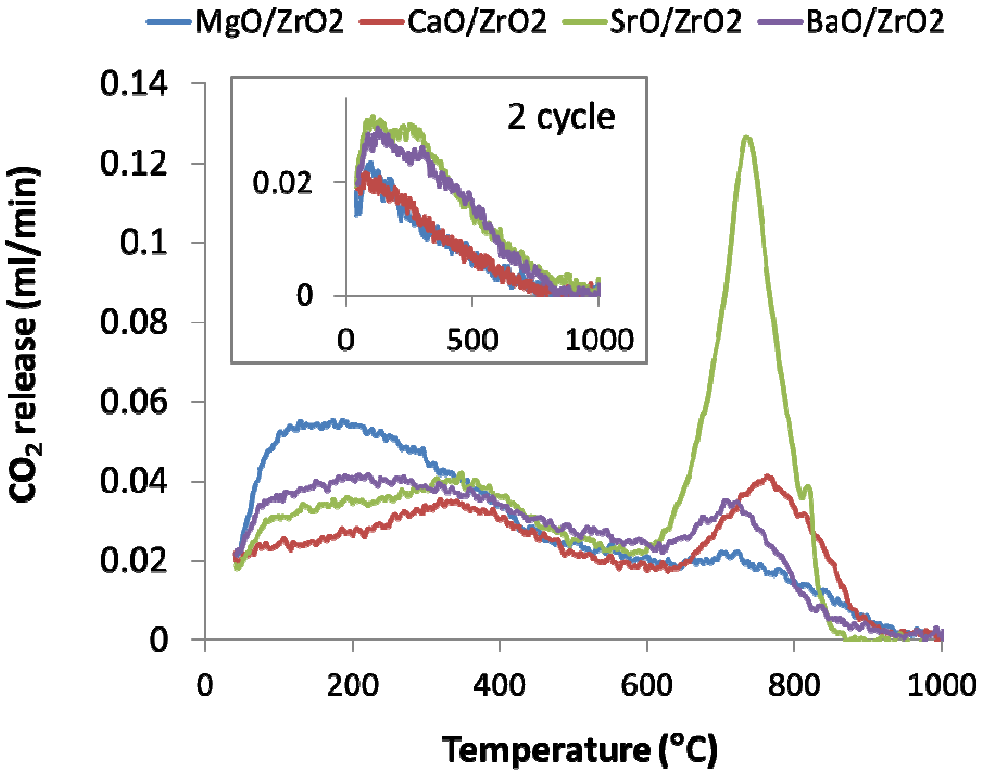

Figure 8 TPD of alkaline earth metal oxides on ZrO_2. In the inset the second desorption is displayed in cyclic adsorption/desorption experiments

Interestingly the position of the high temperature desorption peak seems independent of the nature of the metal ion and the peak is for all samples located between 750-800 °C. The intensity of this peaks varies but in a non-systematic way through MgO<BaO<CaO<SrO. No correlation between the ionic ratio of the metal and the performance as CO_2 capture material could be established. We believe that this is related to strong metal-oxide-zirconia interaction though more study is needed to understand the phenomenon in detail. It was also investigated if the ZrO_2 supported alkaline earth metal oxides could be reused for a second adsorption/desorption cycle. The desorption profiles are shown in the inset in Figure 8. A disadvantages of the zirconia system is seen when comparing the first and the second desorption cycle – and almost no CO_2 is desorbed in the 2. cycle. This can be explained by the fact that the material properties has changed dramatically by the heat treatment to 1000 °C. This is

indicated by the phase transition observed by XRD already beginning at 800 °C (Figure 4) also resulting in less available base sites than after heat treatment at 600 °C (Table 1). This challenge can most likely be overcome by regenerating the material at lower temperature e.g. 700 °C for a longer period of time.

3.3.4 Conclusions

We have shown that zirconia is an interesting support for CaO used for post combustion applications. The preparation method is important for the distribution of strong/weak base sites and thus for de desorption of CO_2 important for regeneration. By desorbing CO_2 at too high temperature (800 °C and higher) the material properties changes (phase transition) and the CO_2 capacity decreased. It is thus important to optimize the regeneration condition ea. investigate possibilities for CO_2 desorption in isothermal period of 600-700 °C.

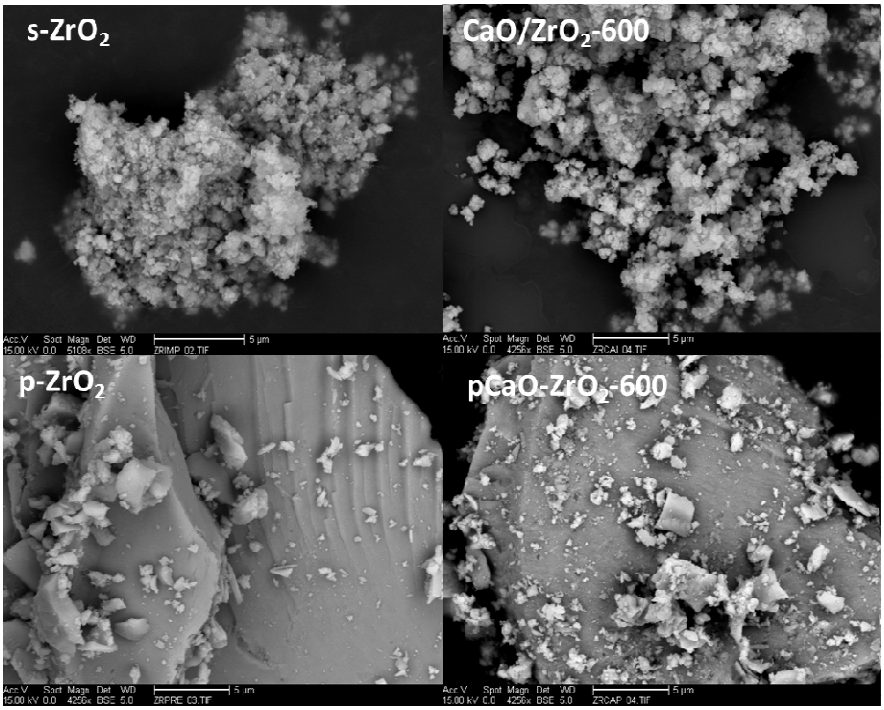

Figure S1. SEM of ZrO_2, ZrO_2 precip and CaO/ZrO_2 and $CaO\text{-}ZrO_2$

All Ca-containing samples displayed similar morphologies as the bare supports.

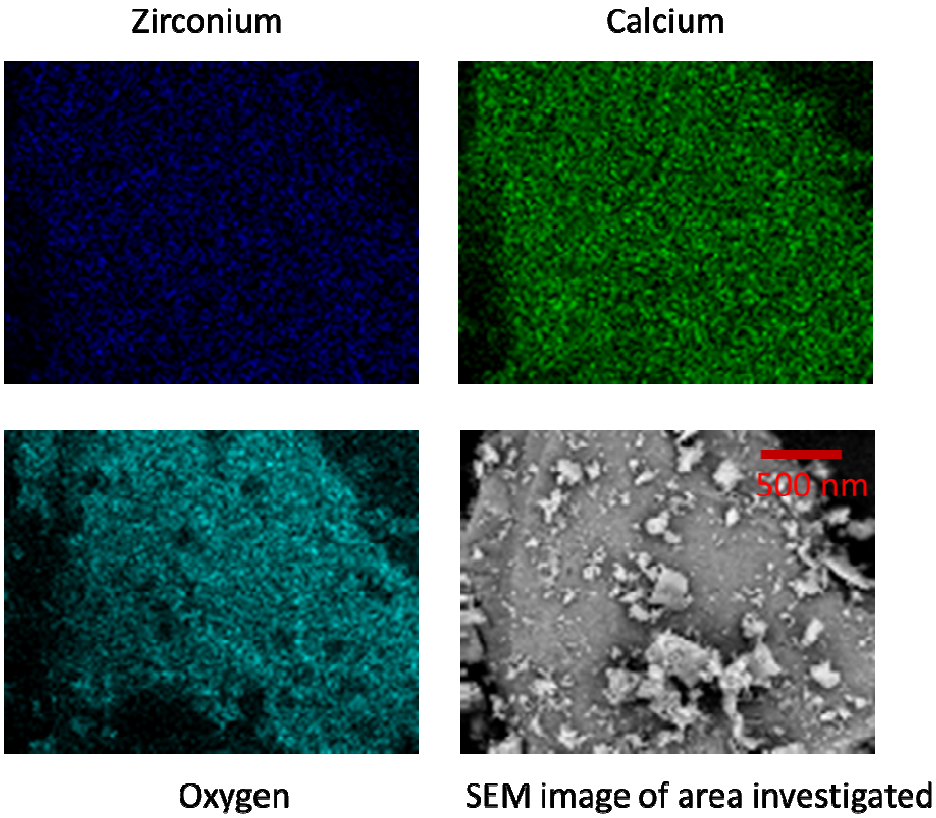

Figure S2. SEM and element mapping of $CaO\text{-}ZrO_2$ showing a homogeneous distribution of Ca and Zr.

3.4 Summary and Conclusions

It has been clearly demonstrated that steam hydration of a CaO-based material is effective in improving the carrying capacity of a sorbent. However the steam consumption needed for the extra capacity is not significantly lower than other CCS technologies and may even be substantially higher. Steam hydration requires adding a steam equivalent of 1-2 moles steam per mol Ca present, which would correspond to complete conversion to $Ca(OH)_2$ during the hydration step. This however does not fully activate the Ca-based material as a maximum of only 30% of the Ca is available for CO_2 capture in the next cycle. The mechanistic understanding of how dopants improve long term stability would seem to offer more hope in understanding how these systems can be made more competitive. Consequently the focus of this work shifted to the understanding of both dopants and the effect of support on the activity of these materials.

Magnesium seems to have a promising effect for stability and the possibility for regeneration in the sol gel method, but when impregnating it to commercial CaO the stabilizing effect was no longer apparent. The location of Mg must thus be considered crucial for the impact on the performance of CaO CO_2 capture materials. This would require substantial extra work on identify the mechanism by which such stabilisation could take place, and it is very much the question if this could necessarily lead to a performance in improvement that was justified by the costs involved.

Finally, zirconia was shown to be an interesting support for CaO used for post combustion applications. The preparation method is important for the distribution of strong/weak base sites and thus for de desorption of CO_2 important for regeneration. However, by desorbing CO_2 at too high temperature (800 °C and higher) the material properties changes (phase transition) and the CO_2 capacity decreased. The most obvious solution to use this new sorbent would be to optimise the regeneration conditions. However, it is known that lower temperature regeneration of CaO-based sorbent will lead to inefficiencies in the overall post-combustion process, because this will drive up steam demands and the partial pressure of CO_2 will remain low under such regeneration conditions.

The project has increased the knowledge of CaO-based material with both H_2O and CO_2 under post combustion conditions. Of the solutions available, the use of steam to increase the cyclic capacity of these materials would seem to be the most applicable for near term use, unless new system configurations can be devised to take advantage of the cyclic capacity of zirconia supported materials below their transition point.